Earth-Science Reviews 278 (2026) 105516

Contents lists available at ScienceDirect

Earth-Science Reviews

journal homepage: www.elsevier.com/locate/earscirev

Review Article

Origins of the Mg/Li ratio in closed-basin brines of the Lithium Triangle: The relative importance of high- and low-temperature water-rock interactions

Gordon D.Z. Williams, Avner Vengosh *

Division of Earth and Climate Science, Nicholas School of the Environment, Duke University, United States of America

A R T I C L E I N F O

Keywords:
Lithium
Magnesium
Central Andes
Brine
Geothermal

A B S T R A C T

The Mg/Li ratio is widely used to evaluate the extraction potential of lithium-rich brines, yet the processes controlling its variability remain poorly constrained. Across the Lithium Triangle of the Central Andes in South America, closed-basin brines exhibit Mg/Li ratios spanning more than three orders of magnitude (from <1 to >500) despite broadly similar geology, evaporative evolution, and major-ion chemistry. Here we present a regional synthesis of Mg/Li ratios in spring waters and closed-basin brines, drawing on geochemical data for hundreds of springs ($n = 577$) and brines ($n = 1078$) from more than 100 closed-basins to develop a framework for interpreting Mg/Li variability. We show that Mg/Li ratios in inflow waters are primarily governed by the temperature of water-rock interactions: high-temperature geothermal systems produce low Mg/Li ratios, whereas low-temperature, near-surface water-rock interactions produce water with higher Mg/Li ratios, resembling the ratios in source rocks. At the basin scale, brine Mg/Li ratios reflect mixing-weighted integration of high- and low-temperature derived inflows. Evaporative concentration, mineral precipitation, and water-sediment interactions modify absolute solute concentrations but generally preserve the integrated Mg/Li ratios of the inflows under the circumneutral pH conditions typical of Lithium Triangle brines. Important exceptions occur in alkaline systems, where Mg-silicate precipitation alters the inflow Mg/Li signature. These results demonstrate that Mg/Li ratios record the integrated thermal history of solute sources and provide a context-dependent indicator of geothermal versus near-surface fluid contributions to closed-basin brines. This framework refines interpretation of Mg/Li ratios in lithium exploration and has broader implications for continental brine systems worldwide.

Contents

* Corresponding author.
E-mail address: vengosh@duke.edu (A. Vengosh).

https://doi.org/10.1016/j.earscirev.2026.105516
Received 19 February 2026; Received in revised form 28 March 2026; Accepted 19 April 2026
Available online 20 April 2026

1. Introduction

Lithium (Li) is a critical element for the global clean energy transition due to its essential role in Li-ion batteries used in electric vehicles and grid-scale energy storage (IEA, 2021). Lithium is produced primarily from two deposit types: hard-rock Li-rich pegmatites and closed-basin Li-rich brines (Kesler et al., 2012). Although closed-basin brines host the majority of the world's Li resources (Kesler et al., 2012), they currently account for only ~40% of global production (Jaskula, 2025a; Moon, 2025). A series of over 100 such closed-basins occur in the high Central Andes, collectively hosting nearly 50% of global Li resources in a region known as the Lithium Triangle, spanning parts of Chile, Argentina, and Bolivia (Fig. 1) (Jaskula, 2025a; Kesler et al., 2012; Mihalasky et al., 2020; Munk et al., 2025). Several of these basins are actively producing Li, while many others are under exploration or development, making the Lithium Triangle one of the most important

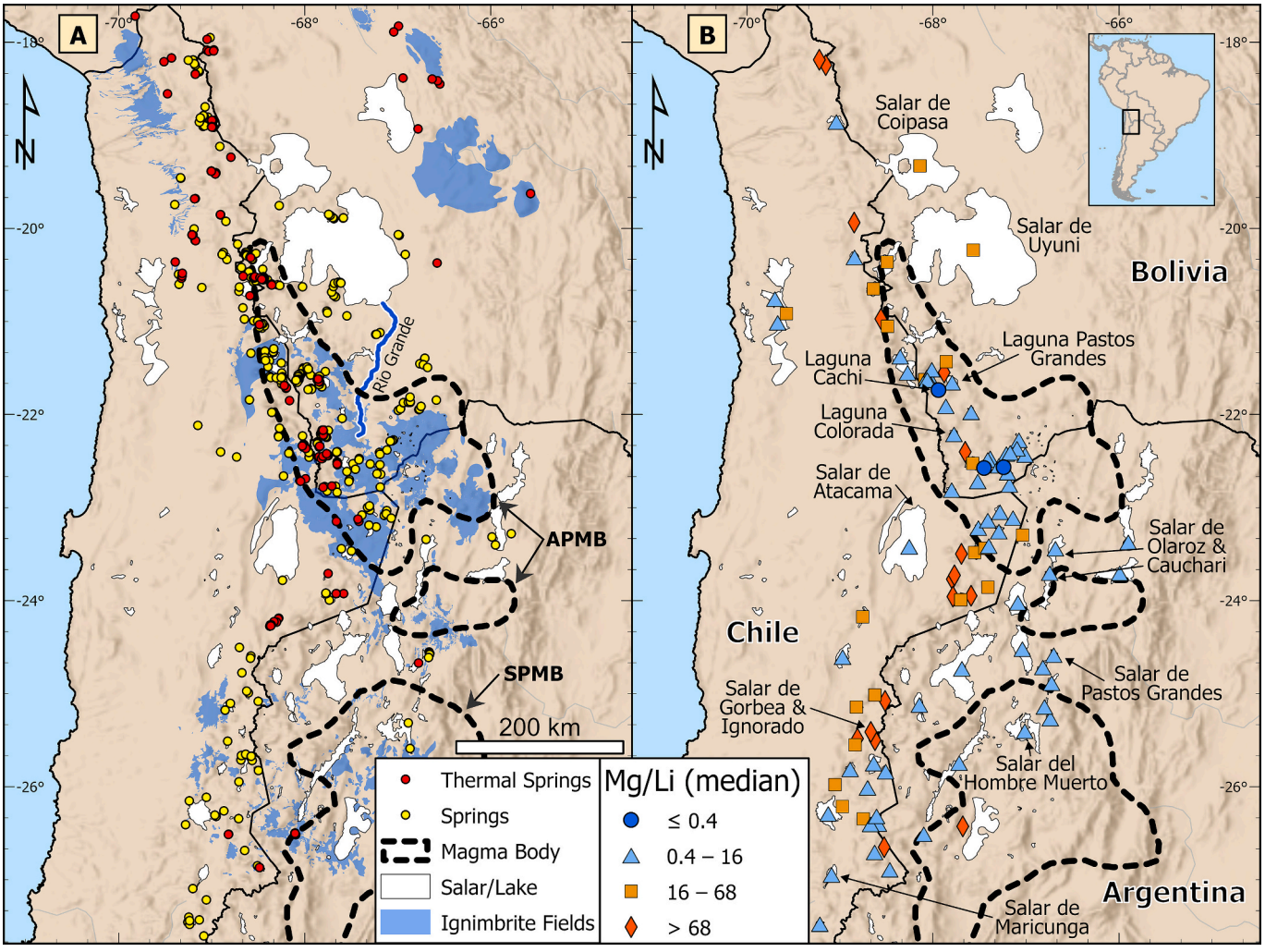

Fig. 1. Maps of the Lithium Triangle in the Central Andes, panels A and B are the same geographic extent. (A) Map of cold and thermal spring waters (not all datapoints have location information) from the compiled dataset evaluated in this study and their relationship to the large ignimbrite fields of the Central Andes, the Altiplano-Puna Magma Body (APMB), the Southern Puna Magma Body (SPMB), and closed-basin salars/lakes. (B) Map of the median Mg/Li ratio (from the compiled dataset) in the closed-basin brines/waters from salars/lakes of the Lithium Triangle (the symbol is larger than the visible surface area of most closed-basins), ranges in values that were determined following the classification scheme described in the text (section 3.1). Several notable salars/lakes and those discussed in the text are labeled. Map layers modified from several sources: Ignimbrites (Freymuth et al., 2015), Salars (Mihalasky et al., 2020), APMB (de Silva et al., 2006), SPMB (Ibarra and Prezzi, 2019).

regions for future Li supply (Jaskula, 2025b).

A key geochemical parameter controlling the economic viability of Li brines is the co-occurrence of magnesium (Mg), as Mg interferes with Li extraction due to its similar ionic radius and chemical behavior (Kesler et al., 2012; Munk et al., 2025). Consequently, the Mg/Li ratio has long been used as a first-order screening criterion in Li-brine exploration and resource evaluation. High Mg/Li ratios increase processing costs and chemical consumption for Mg removal, posing challenges for both conventional evaporative extraction and emerging direct Li extraction (DLE) technologies (Meshram et al., 2014; Mojid et al., 2024; Stringfellow and Dobson, 2021; Yang et al., 2024; Zhu et al., 2023). As a result, brines with Mg/Li ratios below ~10 are generally considered more favorable for Li extraction (Munk et al., 2025). For example, the Salar de Atacama in Chile, the world's most productive Li brine, has a Mg/Li ratio of ~7 (López Steinmetz and Salvi, 2021), whereas the Salar de Uyuni in Bolivia, the world's largest Li-brine deposit (Jaskula, 2025a; YLB, 2019), has a substantially higher ratio of ~22 and has long been regarded as difficult to exploit (An et al., 2012; Bradley et al., 2013; López Steinmetz and Salvi, 2021; Meshram et al., 2014).

Despite its widespread consideration, the geochemical origins of the Mg/Li ratio in closed-basin brines remain poorly constrained. Across the Lithium Triangle, Mg/Li ratios span more than three orders of magnitude, from <1 (e.g., Salar de Ratones, Argentina) to >500 (e.g., Salar de Michincha, Chile), yet variations in the Mg/Li ratio show no clear geographic pattern (López Steinmetz and Salvi, 2021). This variability is striking given that most Lithium Triangle brines share broadly similar Na-Cl-(SO_4) chemistries and evolve through comparable evaporative pathways involving calcite, gypsum, ulexite, and halite precipitation, producing largely circumneutral pH brines with occasional calcium (Ca) or Mg enrichment (López Steinmetz and Salvi, 2021; Lowenstein and Risacher, 2009; Risacher and Fritz, 2009; Williams et al., 2025a, 2026). The processes responsible for this heterogeneous and differential enrichment of Mg relative to Li therefore remain unresolved.

Lithium enrichment in the source rocks of the Lithium Triangle is commonly attributed to crustal thickening, volcanism, and post-eruptive cooling which promote Li enrichment in ignimbrites, volcanic glass, and related lithologies (Bradley et al., 2013; Chen et al., 2020; Ducea et al., 2026; Ellis et al., 2018). Leaching of these rocks during water-rock interactions can liberate Li into solution (Álvarez-Amado et al., 2022b; Cortes-Calderon et al., 2025; Del Bono et al., 2026; Ellis et al., 2022; Hofstra et al., 2013; Munk et al., 2018). In addition, geothermal fluids enriched in Li through high-temperature water-rock interactions and magmatic inputs have been proposed as important contributors to Li brines (Alam and Muñoz, 2024; Araoka et al., 2014; Bradley et al., 2013; Ducea et al., 2026; Liu et al., 2025; Sanjuan et al., 2022). The Lithium Triangle lies within the Central Volcanic Zone (CVZ) of the Andes, which hosts extensive ignimbrite fields and large magma bodies such as the Altiplano-Puna Magma Body (APMB) and a series of smaller magma bodies (e.g., the Cerro Galán and Incahuasi magma bodies) collectively known as the Southern Puna Magma Body (SPMB; Fig. 1) (Bertin et al., 2025; de Silva et al., 2006; de Silva, 1989; Schnurr et al., 2007). These features provide heat for regional geothermal systems that may enhance Li mobilization and contribute solutes to closed-basin systems (Cortes-Calderon et al., 2025; Peralta Arnold et al., 2017; Risacher et al., 2011).

At the same time, low-temperature, near-surface water-rock interactions with local andesitic to dacitic volcanic rocks supply solutes to surficial waters (i.e., shallow groundwater, rivers) that flow into the closed basins and are typically relatively dilute waters (Risacher and Fritz, 1991a, 2009). While these waters are relatively dilute, such low-temperature water-rock interactions have also been suggested as a potentially important source of Li to closed-basin brines (Coffey et al., 2021; Ellis et al., 2022; Hofstra et al., 2013). High-temperature geothermal waters, on the other hand, are typically more saline and are in part derived from either the dissolution of ancient evaporites or from the leakage of closed-basin brines (Risacher et al., 2011; Risacher and Fritz, 2009). Although many Lithium Triangle brines are thought to receive at least some geothermal inputs (e.g., Cortes-Calderon et al., 2025; Godfrey and Álvarez-Amado, 2020; Godfrey et al., 2013; Risacher and Fritz, 2009), geochemical and isotopic signatures diagnostic of geothermal origin are commonly overprinted by sedimentary (e.g., δ^7Li fractionation)(Millot et al., 2010) and evaporative processes (e.g., δ^{18}O–δ^2H systematics)(Drever, 1997). As a result, the relative contribution of geothermal water originating from high-temperature water-rock interactions versus inflows originating from near-surface low-temperature water-rock interactions in controlling brine composition has remained difficult to assess.

The Mg-Li geothermometer exploits the preferential incorporation of Mg into secondary minerals at elevated temperatures, resulting in lower Mg/Li ratios in high-temperature fluids (Kharaka and Mariner, 1989). While this relationship is well established in geothermal systems, it remains unclear whether Mg/Li ratios in closed-basin brines primarily reflect the thermal conditions of water-rock interaction at solute sources, or whether they are substantially modified by basin-scale processes such as mixing of multiple inflows (i.e., sources with different Mg/Li ratios), evaporative concentration and mineral precipitation, and water-sediment interactions (i.e., loss of Mg or Li to adsorption, incorporation). Resolving this ambiguity is critical for interpreting Mg/Li ratios as indicators of brine genesis and for constraining the ultimate sources of Li to closed-basin brines.

Here we present a regional synthesis of Mg/Li ratios in springs and closed-basin brines across the Lithium Triangle, drawing on geochemical data from hundreds of spring waters and more than 100 closed-basins. By integrating spring water chemistry, brine compositions, and case studies of the geochemical evolution of inflow waters to closed basins, we develop a framework for interpreting Mg/Li ratios in continental closed-basin brine systems. We evaluate the extent to which Mg/Li ratios record the thermal history of solute sources, assess how basin-scale mixing and sedimentary processes modify this signal, and identify the conditions under which Mg/Li ratios retain or lose diagnostic value. This framework provides new constraints on the role of geothermal versus near-surface inputs in Li-brine formation and offers a revised perspective on one of the most widely used geochemical indicators in Li exploration.

2. Materials and methods

2.1. Data compilation

Data for inflows and brines were compiled from numerous sources with samples from around the Lithium Triangle (Alam and Muñoz, 2024; Álvarez-Amado et al., 2022b; Ávila Salas, 2023; Badaut and Risacher, 1983; Borda et al., 2023; Cortecci et al., 2005; Ericksen et al., 1978; Ericksen and Salas, 1987; Gamboa et al., 2019; Garcia et al., 2020; Godfrey and Álvarez-Amado, 2020; Godfrey et al., 2013; Grove et al., 2003; Haferburg et al., 2017; Ide, 1978; Kasemann et al., 2004; Lagos Durán, 2016; López Steinmetz, 2017; López Steinmetz et al., 2018, 2020; Meixner et al., 2022; Moraga et al., 1974; Morteani et al., 2014; Muller et al., 2020; Munk et al., 2018, 2021; Placzek, 2005; Placzek et al., 2011; Pueyo et al., 2017, 2021; Rettig et al., 1980; Risacher, 1992; Risacher et al., 1999, 2011; Risacher and Fritz, 1991a, 1991b; Rissmann et al., 2015; Sarchi et al., 2023; Scandiffio and Alvarez, 1990; Scandiffio and Cassis, 1990; Scandiffio and Rodriguez, 1990; Schmidt, 2010; Schmitt et al., 2002; Servant-Vildary and Roux, 1990; Sieland et al., 2011; Sieland, 2014; Tassi et al., 2010; Vignoni et al., 2024; Williams et al., 2025a, 2026; Williams and Vengosh, 2025). This amounts to over 3000 individual samples of which 577 are from springs and 1068 from brines across 103 closed basins with both reported Mg and Li concentrations. Data for numerous other springs, rivers, and streams in the region and other analytes including major elements, trace elements, and isotopes were also compiled and are available in this dataset, however, are not the focus of this study. Geographic coordinates were not available for all samples, however when available it was compiled or

approximated and digitized from maps. The entire dataset can be found in the supplementary information and any updated versions at https://gordondzwilliams.github.io/LTdataset.

The spring waters considered in this study were classified as either cold springs or thermal springs. Thermal springs were classified as such if their field measured temperature was ≥30 °C or if they were classified as thermal springs in their original publication. Cold springs followed the same protocol but for field measured temperatures <30 °C. This 30 °C cutoff was chosen since it is the lower limit of the applicable temperature range for the geothermometer of Kharaka and Mariner (1989), which is an indicative parameter as discussed in section 3.1. Any uncategorized springs without a reported temperature were only considered in the total distribution of Mg/Li ratios in spring waters. Brines are classified as from within the closed basin if they were originally reported as representative of the brine or if they are the only datapoint available. In several cases, brines along the margins of a salar were not considered representative if they appeared to be directly fed by local inflows. This was notably the case with the Salar de Atacama where numerous brine pools along the margin of the salar are fed by or mixed with dilute inflows, thus only brines from within the central region/halite nucleus were considered in this study.

The rock geochemical data used is from the database of Mamani et al. (2010) covering the Central Andes and was cleaned to only include samples with both reported Mg and Li concentrations and to only include samples from within the Lithium Triangle countries of Chile, Bolivia, and Argentina.

2.2. Analytical methods & sample collection

In addition to the compiled dataset, new samples were collected along a transect of the Rio Grande stream as it flows down from the APMB towards the Salar de Uyuni and within the Uyuni watershed (n = 24); a single brine sample from the Salar de Coipasa (n = 1) was also collected. The analytical and sample collection methods and analytical validation for brines and waters can be found in Williams et al. (2026, 2025b, 2025a) with discussion of analytical accuracy and error found in Williams et al. (2025a). Briefly, for cations and trace elements, samples were collected in acid washed HDPE bottles and acidified to pH <2 while for anions and alkalinity were collected in rinsed HDPE bottles without headspace. All samples were filtered to 0.45 μm. All brines and waters were measured for major cations (Li, Na, Mg, Ca) and major anions (Cl, Br, SO_4) via ion chromatography (IC) on Thermo Scientific Aquion IC and Dionex IC DX-2100 systems, respectively. Trace elements including Li (if the analytical concentration was <1000 μg/L) and B were measured with a Thermo Fisher Scientific X-Series II inductively coupled plasma mass spectrometer at Duke University. Alkalinities were measured only in freshwater via titration to pH 4.5 using 0.02 M HCl. The recovery for all elements measured was within ±6% of the expected value the IAPSO Atlantic Seawater Standard, which was prepared and analyzed in the same manner as all samples.

3. Origins and modification of the Mg/Li ratio in waters and brines

Mg and Li are widely recognized to substitute for each other in mineral surfaces and structures during water-rock interactions. The degree of this substitution is temperature dependent and has been characterized in both low-temperature (e.g., the Mg/Li paleo-seawater temperature proxy in marine carbonates)(Bryan and Marchitto, 2008; Case et al., 2010; Dellinger et al., 2018) and high-temperature systems (e.g., the Mg-Li geothermometer in sedimentary basin and geothermal fluids)(Kharaka and Mariner, 1989), where higher temperatures preferentially incorporate Mg into mineral phases. In geothermal systems, Mg has long been known to preferentially incorporate into (secondary) mineral phases at higher temperatures relative to alkali metals (Giggenbach, 1988; Nicholson, 1993), while Li is typically considered one of the most conservative elements (Nicholson, 1993). Since the relationships between Mg and Li are temperature dependent and both Mg and Li are generally considered conservative ions in evaporative systems of the Lithium Triangle, we hypothesize that the Mg/Li ratio of closed-

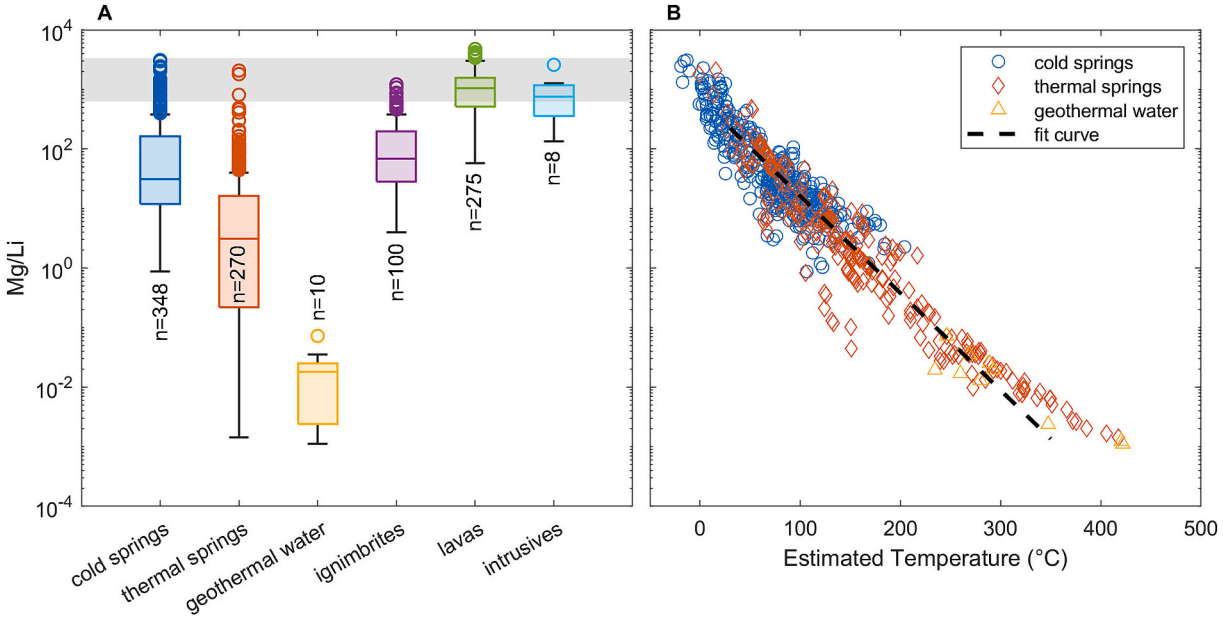

Fig. 2. (A) Variations in Mg/Li ratios of spring waters and volcanic rocks across the Lithium Triangle. Cold springs overlap with the full range of regional rock compositions, whereas thermal springs and deep geothermal waters typically exhibit substantially lower Mg/Li ratios. Rock geochemical data are from the database of Mamani et al. (2010). For reference, the shaded region is the range in mean values for the upper, middle, and lower continental crust (Rudnick and Gao, 2014). (B) Estimated equilibrium temperatures of water-rock interactions calculated using the Mg-Li geothermometer of Kharaka and Mariner (1989). Although some calculated temperatures fall outside the nominal applicability range of the geothermometer (30–350 °C), a strong inverse relationship is observed between Mg/Li ratio and estimated temperature, highlighting the systematic dependence of Mg/Li ratios on the thermal conditions of water-rock interaction. All fluid data are from the compiled dataset.

basin brines is preserved from its original solute source(s) and can be used to determine the types of inflows providing solutes to closed-basin brines (i.e., geothermal versus low-temperature near-surface inflows). The following sections investigate the variations between the Mg/Li ratio in waters from low- and high-temperature systems in the Lithium Triangle and how these original ratios can be modified as a water flows into a terminal basin. This includes mixing of different water sources, evaporation and mineral precipitation, and uptake of ions through water-sediment interactions.

3.1. Cold springs versus thermal waters

Using a compiled dataset, we evaluated data from cold springs (<30 °C, $n = 348$) and thermal springs (≥30 °C, $n = 270$) from throughout the Lithium Triangle (Fig. 1A) combined with a small dataset of deep geothermal waters ($n = 10$) that are samples collected from geothermal wells without a direct connection to the surface. Fig. 2A shows the considerable ranges in these values; the median Mg/Li ratio for cold spring is ~31, thermal springs ~3, and deep geothermal waters ~0.02. By comparison, volcanic rocks of the Central Andes (Mamani et al., 2010) typically have much higher Mg/Li ratios with median values for ignimbrites at ~68, lavas at ~1050, and some intrusive igneous rocks at ~750 (Fig. 2A). For reference, the Mg/Li ratios of the bulk continental crust (mean values for upper middle and lower crust) ranges from ~623 (upper crust) to ~3358 (lower crust) (Rudnick and Gao, 2014), generally overlapping with non-ignimbrite rocks (Fig. 2A). Waters from each group typically have lower Mg/Li ratios than the host rocks and bulk continental crust ($p < 0.001$, Fig. 2A), suggesting that Li is preferentially mobilized into the aquatic phase.

Experimental leaching studies with a variety of rock types and under different low- and high-temperature conditions ranging from 25 to 400 °C have previously demonstrated that under low-temperature conditions the aqueous Mg/Li ratios typically mimic that of the initial source rocks (Yuan et al., 2021). High-temperature leaching, on the other hand, leads to much lower Mg/Li ratios than the source rocks, in agreement with known trends in geothermal systems (Yuan et al., 2021). This is clearly the case in spring waters throughout the Lithium Triangle; cold spring waters have an overlapping range of Mg/Li ratios with the different rock types found in the Lithium Triangle and the bulk continental crust while thermal springs and deep geothermal waters typically have much lower values (Fig. 2A).

While the measured temperature of spring waters at the surface may not reflect their temperature at depth, the original equilibrium temperature at depth can be reconstructed using chemical geothermometers. This is done using variations in chemical concentrations or ratios that have been calibrated to reflect equilibrium temperatures at depth. To estimate the reservoir temperature we use the Mg-Li geothermometer of Kharaka and Mariner (1989), which reportedly estimates subsurface temperatures between 30 °C and 350 °C. The equation is:

$$T(^{\circ}\mathrm{C}) = \frac{2200}{\log\left(\frac{\sqrt{Mg}}{Li}\right) + 5.47} - 273 \quad (1)$$

where Mg and Li are the concentration in mg/L and T represents the equilibrium reservoir temperature. It should be noted that the calculated temperatures are estimates and that other factors such as rock type and fluid composition can influence the accuracy of chemical geothermometers (Cioni and Marini, 2020); the Mg-Li geothermometer, however, has generally proven reliable in different rock types and in fluids with high Li concentrations (Boschetti et al., 2024; Kharaka and Mariner, 1989), conditions relevant to the geothermal waters of the central Andes (Cortecci et al., 2005; Inostroza et al., 2025; Peralta Arnold et al., 2017; Risacher et al., 2011). Accordingly, we focus on the Mg-Li geothermometer in this study, and evaluation of alternative geothermometers is beyond the scope of this study.

Since Eq. (1) is concentration dependent, it is not directly a function of the Mg/Li ratio alone. Nonetheless, plotting estimated reservoir temperatures against the Mg/Li ratios of cold springs, thermal springs, and deep geothermal waters reveals a strong inverse correlation ($\rho = 0.92$, $p < 0.001$; Fig. 2B), indicating that Mg/Li ratios systematically decrease with increasing temperature of water-rock interaction.

To illustrate this relationship using Mg/Li ratios alone, independent of absolute concentrations, we fit an exponential curve to the data within the reported applicability range of the Mg-Li geothermometer (30–350 °C) (Fig. 2B). This yields the following empirical relationship:

$$\frac{Mg}{Li} = 688.6 * e^{-0.03755 * T(^{\circ}\mathrm{C})} \quad (2)$$

This relationship explains a substantial portion of the variance in the data ($R^2 = 0.53$), but it should be emphasized that Eq. (2) is not intended as a predictive geothermometer. Rather, it provides a heuristic framework for visualizing how Mg/Li ratios broadly vary as a function of the temperature of water-rock interactions across diverse lithologies and fluid compositions. The remaining variance likely reflects differences in host rock composition, fluid evolution, mixing of multiple water sources, and post-equilibration processes.

Experimental studies demonstrate that low-temperature leaching of volcanic rocks typically produces aqueous Mg/Li ratios similar to those of the source lithology, whereas higher-temperature interactions preferentially sequester Mg into secondary minerals while Li remains relatively conservative (Yuan et al., 2021). Consistent with this behavior, ignimbrites of the Central Andes, which are widely considered a primary source of Li to regional waters (Álvarez-Amado et al., 2022b; Álvarez-Amado et al., 2022a; Cortes-Calderon et al., 2025; Del Bono et al., 2026; Meixner et al., 2022; Munk et al., 2018; Risacher and Fritz, 2009), have a median Mg/Li ratio of ~68 (Fig. 2A). Other common lithologies in the region, including lavas and intrusive igneous rocks, typically exhibit even higher Mg/Li ratios that are similar to the bulk continental crust (Fig. 2A). On this basis, we consider waters derived predominantly from low-temperature (near-surface) water-rock interactions to have Mg/Li ratios similar to or greater than those of ignimbrites (i.e., > ~68). Using Eq. (2) solely as a qualitative guide, Mg/Li ratios of ~16 and ~ 0.4 broadly align with equilibrium temperatures on the order of ~100 °C and ~200 °C, respectively.

Accordingly, we classify Mg/Li ratios in waters as indicative of dominantly influenced by low-temperature (>68), moderate-temperature (68–16), high-temperature (16–0.4), or very-high-temperature (<0.4) water-rock interactions. These categories are intended to represent broad thermal regimes rather than discrete temperature thresholds and are used below to facilitate regional comparison of Mg/Li ratios in closed-basin brines.

3.2. Modification of the Mg/Li ratio in inflow waters

While geothermal waters that reach the (near)-surface environment may retain the Mg/Li ratio they achieved at depth, surficial processes can potentially modify it. Potential modification mechanisms include (1) mixing of different water sources, (2) precipitation or dissolution of Mg or Li bearing minerals, and (3) retention of Li and Mg during water-sediment interactions (e.g., adsorption to clay and/or oxides).

The evaporative evolution of dilute inflow waters to closed-basin brines leads to the precipitation of several primary minerals. In the Lithium Triangle these are dominantly calcite ($CaCO_3$), gypsum ($CaSO_4 \bullet xH_2O$), ulexite ($NaCaB_5O_9 \bullet xH_2O$), and halite (NaCl) (Risacher and Fritz, 2009; Williams et al., 2026), which are not expected to appreciably incorporate Li and Mg as substituting ions (Bąbel and Schreiber, 2014; McCaffrey et al., 1987). Notably Mg salts like polyhalite only form from extremely evaporated hypersaline brines and are rare in the natural settings (Williams et al., 2026). Lithium-bearing salts like Li-sulfate have been hypothesized to form from the extreme

evaporation of natural brines (Boschetti et al., 2007) and are known to form in evaporation ponds (Williams and Vengosh, 2025), but have not been found or proven to form naturally in salar systems.

In general the precipitation of Mg-silicates (e.g., sepiolite, clays) and Mg-carbonates from inflow waters and brines, a process analogous to reverse weathering involving authigenic clay formation, are known to be important steps in controlling the aqueous geochemistry of brines (Eugster and Hardie, 1978; Hardie and Eugster, 1970; Tosca and Tutolo, 2023). Their precipitation, however, is primarily controlled by pH where alkaline conditions (pH > ~9) facilitate their formation and thus they are typically found in alkaline lakes (Tosca and Tutolo, 2023; Tutolo and Tosca, 2018). Such alkaline conditions are however not common to closed-basin brines or inflows during their evaporative evolution in the Lithium Triangle (Risacher et al., 2003; Risacher and Fritz, 2009). This is in part as a result of the oxidation of aeolian sulfur/sulfides (Risacher and Fritz, 2009; Risacher and Fritz, 1991a) and the enhanced dissociation of boric acid at high salinities (Williams et al., 2025a), which inhibit the formation of alkaline brines and generally produce a circumneutral pH brine. Furthermore, the cold and arid conditions of the Lithium Triangle and the generally low Al concentrations in waters have been argued as inhibiting the authigenic formation of clays (Godfrey et al., 2019; Godfrey et al., 2013; Risacher, 1984). Despite this, authigenic Mg-smectites have been observed to significantly and actively form on biogenic silica but only in a few alkaline salars of Bolivia (Badaut and Risacher, 1983). Independent Mg-carbonates (i.e., magnesite) are typically undersaturated in waters from the Lithium Triangle and are not expected to form (Risacher and Fritz, 2009), however, relatively minor Mg incorporation as a substitute for Ca in calcite can occur (Vignoni et al., 2024). From this we can reasonably expect that Mg and Li are not appreciably removed from solution by the precipitation of salts or Mg-silicates in the Lithium Triangle.

To assess how the Mg/Li ratio can be modified, we consider four different closed basin systems with different Mg/Li ratios and geological settings: (1) Laguna Pastos Grandes, which has a brine dominantly derived from geothermal waters; (2) the Salar de Uyuni (SDU), which has a brine derived from multiple sources and has a relatively large river and delta system where evaporite minerals precipitate and waters interact with detrital sediments; (3) the Laguna Colorada, which is one of the few (moderately) alkaline brines in closed-basins of the Lithium Triangle with the formation of Mg-silicates; and (4) the Salars de Gorbea and Ignorado, the only two known acid brines in closed-basins of the Lithium Triangle.

3.2.1. *The Laguna Pastos Grandes, a high-temperature system*

The Laguna Pastos Grandes (LPG) in Bolivia is a relatively small playa/salt flat (~125 km^2) (Risacher and Fritz, 1991a), is primarily fed by thermal springs that discharge within and around the playa/salt crust, and is situated within the APMB (Fig. 1) (Ballivian and Risacher, 1981; Bougeault et al., 2020; Jones and Renaut, 1994; Muller et al., 2020; Risacher and Eugster, 1979). Consequently, the LPG represents a brine with a clear geothermal connection and yet it also has many of the same geochemical characteristics that occur in other salars. All major evaporite salts forming at other salars are also forming at LPG from the evaporation of inflowing thermal spring water including, calcite, gypsum, ulexite, and halite (Muller et al., 2020; Risacher and Eugster, 1979), while the conditions (pH ~ 7.5) are not suitable for Mg-silicate formation (Badaut and Risacher, 1983). Furthermore, this salar maintains a low δ^7Li value in the brines at ~3.9‰ that essentially mirrors the Li isotope composition of the inflowing thermal springs ranging from 2.6‰ to 5.6‰ (Muller et al., 2020). The low and overlapping δ^7Li values of the brine and thermal springs demonstrates that Li isotopes have not been fractionated, and therefore Li was not retained by sediments (i.e., Li isotope fractionation is expected if Li is retained), meaning that Li maintains its conservative nature during evaporation and mineral precipitation. Given the geochemical similarities between Li and Mg and the cooling of thermal waters at the surface, one would not expect that

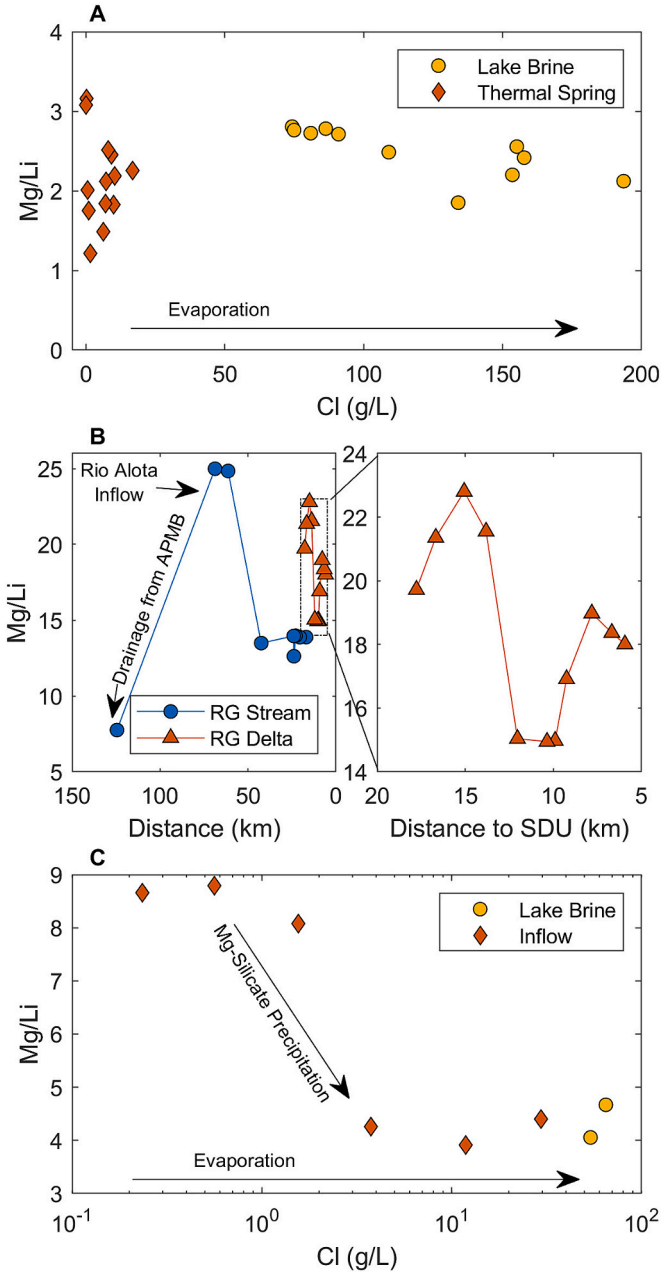

Fig. 3. (A) Mg/Li ratios in Laguna Pastos Grandes, Bolivia and inflowing thermal springs. The Mg/Li ratio of these brines is essentially unaffected by evaporation and mineral precipitation and is directly connected to the thermal springs. Data from the compiled dataset. (B) Evolution of the Mg/Li ratio in the Rio Grande stream (RG Stream) and the Rio Grande delta (RG Delta) with respect to linear distance from the SDU's salt crust. Mixing in the Rio Grande stream alters the Mg/Li ratio from its original value and reflects the weighted integration of different tributaries. Variations in Mg/Li in the RG delta are modified by attenuation of Mg and Li to sediments (see text and Fig. 4 for further discussion). Data from Risacher and Fritz (1991b) and Risacher (1992). (C) Evolution of the Mg/Li ratio in an evaporative transect of a representative inflow to the Laguna Colorada demonstrating the modification of the Mg/Li ratio of inflow waters by Mg-silicate precipitation. Data from Risacher and Fritz (1991a).

Mg is also retained to sediments, similar to Li. This is consistent with variations in the Mg/Li ratio; in the thermal springs the Mg/Li ratio ranges from 1.2 to 3.2 while the LPG brines are between 1.9 and 2.8 (Fig. 3A), demonstrating that the Mg/Li ratio of the inflows is preserved. This low Mg/Li ratio is also consistent with high-temperature

geothermal activity following the classification system described in Section 3.1. To further support this we approximate the reservoir temperature for the thermal springs using Eq. (1) from Kharaka and Mariner (1989), which would suggest a reservoir temperature of ~185 °C (median of thermal springs). This is in rough agreement with the estimated temperatures suggested by Muller et al. (2020) ranging from ~150 to 230 °C on the basis of several different geothermometers. Overall, the LPG demonstrates a relatively clear case in which the Mg/Li ratio of a closed-basin brine is dominantly influenced by high-temperature geothermal waters and the original inflow ratio is unmodified by surficial processes such as evaporation and the sequence of salt precipitation. The LPG therefore represents an endmember case in which Mg/Li ratios retain a clear geothermal signature due to minimal mixing and limited sedimentary modification.

3.2.2. *The Salar de Uyuni, a brine of mixed origin*

The Salar de Uyuni (SDU) is the largest salt flat in the world (~10,000 km^2)(Risacher and Fritz, 1991b) and represents a particularly complex case, as its brines are largely the relicts of a series of extensive paleolakes that episodically connected the SDU basin with several northern terminal basins of the Altiplano, including Coipasa and Poopó, and that received overflow from Lake Titicaca to the north (Baker et al., 2001; Placzek et al., 2013; Risacher and Fritz, 1991b; Williams et al., 2026). The large watershed (roughly the entire Altiplano at ~193,000 km^2)(Lehner et al., 2008) feeding these paleolakes likely integrated solute inputs from waters that experienced a wide range of water-rock interaction temperatures. In this context, Mg/Li ratios in the SDU are not expected to reflect a single water-rock interaction source, but rather a mixing-weighted integration of solute sources with distinct thermal histories. Although the Rio Grande is the only major modern inflow to the SDU and southern inflows like the Rio Grande were also a significant contributor of solutes to the paleolakes (Placzek et al., 2011; Risacher and Fritz, 1991b; Williams et al., 2026), it is estimated to have supplied less than 1% of the halite present in the modern salt crust since the last paleolake stage (Risacher and Fritz, 1991b).

The SDU brines have a relatively high Mg/Li ratio of ~22 on average (López Steinmetz and Salvi, 2021), which we interpret as reflecting a mixed solute inventory dominated by contributions from waters that experienced low-temperature water-rock interactions during the paleolake stages, with a smaller and yet non-negligible contribution from higher-temperature geothermal sources. If the SDU brines were derived exclusively from the desiccation of a well-mixed paleolake system, one might expect the Mg/Li ratios of the Salar de Coipasa (SDC), the next highest basin formerly connected to the SDU, to be similar. However, the SDC exhibits a substantially higher average Mg/Li ratio of ~47 (López Steinmetz and Salvi, 2021). This difference likely reflects post-paleolake modification of the SDC brines through continued solute inputs, particularly from the Rio Lauca (Mg/Li ≈ 56), which floods the salar annually and has contributed up to an estimated ~20% of the halite to the SDC salt crust since the last paleolake (Risacher and Fritz, 1991b). The relatively high Mg/Li ratio of the Rio Lauca, combined with its significant salt flux, suggests that ongoing low-temperature solute inputs have shifted the Mg/Li ratio of the SDC to higher values.

Both the SDU and SDC were also historically influenced by overflow from Lake Titicaca, which has a much higher Mg/Li ratio of ~97 (Risacher and Fritz, 1991b), consistent with the fact that it is dominantly recharged by meteoric inputs (Lima-Quispe et al., 2025) and therefore reflects solutes primarily originating from near-surface, low-temperature water-rock interactions. In contrast, the Rio Grande at its discharge to the southern part of the SDU has a much lower Mg/Li ratio of ~18 (Risacher and Fritz, 1991b), potentially reflecting its drainage of regions associated with the APMB (Fig. 1A), where geothermal activity is common (i.e., near the LPG). Taken together, these observations indicate that the Mg/Li ratios of the SDU and SDC brines represent mixtures of solutes derived from multiple inflows with distinct thermal signatures. Paleolake reconstructions suggest that solutes during the final lake stages were supplied primarily from the north via Lake Titicaca and the Rio Lauca and from the south via the Rio Grande (Grove et al., 2003; Risacher and Fritz, 1991b), with southern inputs considered dominant (Placzek et al., 2013; Placzek et al., 2011).

Using the modern Mg/Li ratios of Lake Titicaca (~97), the Rio Lauca (~56), and the Rio Grande (~18), and assuming that these values are representative of their paleolake-stage counterparts, we conduct simplified mass-balance calculations to approximate source contributions to the SDU brines. If the modern SDU brine Mg/Li ratio (~22) approximates the paleolake value, an assumption supported by the near absence of Mg- and Li-bearing salts in the SDU and the negligible contribution of modern solute inputs (Risacher and Fritz, 1991b; Williams et al., 2026), two-endmember mixing between the Rio Grande and the northern inputs suggests that ~89–95% of the Mg and Li in the SDU is derived from the Rio Grande, with only ~5–11% originating from northern sources. This estimate is consistent with independent assessments indicating that the solute inputs from Lake Titicaca were relatively minor (Placzek et al., 2013; Placzek et al., 2011). Importantly, this analysis demonstrates that the Mg/Li ratio of a closed-basin brine reflects the mixing-weighted integration of solute sources with different thermal histories, rather than recording a single source with high- or low-temperature water-rock interactions.

The Rio Grande, the only major modern inflow to the SDU, provides an opportunity to examine how Mg/Li ratios of inflows can evolve during transport, mixing, and evaporation prior to flowing into basin brines. At its headwaters, the Rio Grande drains the APMB (Fig. 1A), a deep-seated magma body that provides heat for regional geothermal systems (de Silva et al., 2006). Near this region, the river exhibits its lowest Mg/Li ratios (~7.7), which increase downstream to ~25, decrease to ~14, and then rise again to ~20 within the Rio Grande Delta (Fig. 3B). These variations are interpreted primarily as the result of mixing with tributaries that experienced different water-rock interaction sources. One major tributary, the Rio Alota, has Mg/Li ratios ranging from ~26 to 43 and Na/Cl molar ratios of ~1.00–1.15, characteristic of relatively low-temperature alteration of local volcanic rocks (Risacher and Fritz, 2009; Risacher and Fritz, 1991a). In contrast, the most upstream Rio Grande sample has a Na/Cl molar ratio of ~0.81, indicative of recycled brines typical of regional geothermal waters (Risacher et al., 2011; Risacher and Fritz, 2009). The initial increase in the Mg/Li ratio of the Rio Grande likely reflects mixing with the Rio Alota downstream of their confluence (Fig. 3B), with subsequent fluctuations attributable to additional tributary inputs. Throughout its course, the Rio Grande remains relatively dilute, with TDS increasing from ~1.4 g/L upstream to ~2.3 g/L prior to entering the delta. Overall, along the flow of ~190 km, the Mg/Li ratio of the Rio Grande is modified from a geothermal fingerprint in the APMB (ratio ~ 7.7) to a more intermediate value or ~ 20 due to inputs from tributaries with low-temperature fingerprints.

Within the Rio Grande Delta, inflowing waters evaporatively evolve to hypersaline compositions, precipitating calcite, gypsum, ulexite, and halite (Risacher and Fritz, 1991b; Williams et al., 2026). During this evolution, waters also interact extensively with detrital sediments before mixing with paleolake-derived brines (Risacher and Fritz, 1991b; Williams et al., 2026). Although Mg- or Li-bearing minerals have not been reported in the delta and conditions are not favorable for Mg-silicate formation due to circumneutral pH (Badaut and Risacher, 1983; Risacher and Fritz, 1991b), Mg/Li ratios in the delta waters/brines vary between ~15 and 23 and converge to ~18 prior to mixing with the SDU brine (Fig. 3B). In the absence of discrete Mg or Li mineral phases, these variations are best explained by partial attenuation of both elements through water-sediment interactions (i.e., adsorption). Lithium isotope data show that δ^7Li values increase from ~3‰ in the river to ~12‰ in the brine (Williams et al., 2026), indicating the removal of Li to sediments and the subsequent Li isotope fractionation. To determine the fraction of Li and Mg removed, we normalize Li and Mg to Br, a relatively conservative element during the evaporation

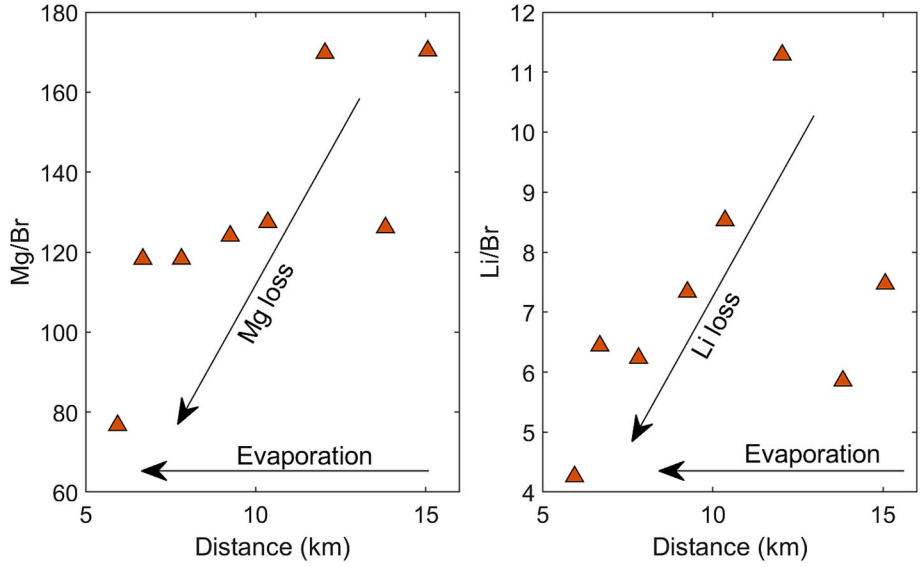

Fig. 4. Variations in the Mg/Br and Li/Br ratios (mass ratios) in the Rio Grande delta as waters interact with sediments. It is clear that both Li and Mg are lost to water-sediment interactions as both decrease with respect to Br, a relatively conservative tracer, along their flow towards the SDU. Distance is linear distance from the SDU prior to any halite precipitation or contact with the salt crust. Data from Risacher and Fritz (1991b) and Risacher (1992).

process. Conducting mass balance calculations between the highest (11.3 and 170) and lowest (4.3 and 77.7) Li/Br and Mg/Br ratios found at respectively early and late stages of evaporation in the delta suggests that ~62% of Li and ~ 55% of Mg are lost to water-sediment interactions (regardless of the manner of attenuation)(Fig. 4). This estimate is consistent with a Rayleigh fractionation calculation using Li isotopic fractionation factors of ~16–20‰, factors, which have been reported for Li uptake into oxides and clays (Vigier et al., 2008; Wimpenny et al., 2015; Wimpenny et al., 2010). Despite this attenuation, our evaluation indicates that Mg and Li are removed to roughly comparable degrees, resulting in the approximate preservation of the integrated Mg/Li ratio that remains ~18 in the final Rio Grande derived brines as compared to the value of ~14 in the stream prior to entering the delta.

Within the classification framework developed in this study, the integrated Mg/Li ratio of the Rio Grande after evaporative evolution falls within the range indicative of moderate-temperature influence, consistent with its mixed solute provenance that includes both high-temperature geothermal inputs from the APMB region and low-temperature near-surface inputs from tributaries such as the Rio Alota. This example demonstrates that while Mg/Li ratios are not static in deltaic environments and both Mg and Li can be significantly attenuated during evaporation and water-sediment interaction, the magnitude of the integrated Mg/Li ratio of the inflow is largely preserved.

In sum, the evolution of the Rio Grande and the paleohydrology of the SDU illustrate that (1) Mg/Li ratios of individual inflows reflect the temperature of water-rock interactions of each source; (2) mixing of these inflows produces composite Mg/Li ratios that record a weighted integration of these thermal signatures rather than discrete interaction temperatures; and (3) evaporative concentration and water-sediment interactions modify the absolute Mg and Li concentrations and yet can roughly preserve the integrated Mg/Li ratio of the inflows. Accordingly, the Mg/Li ratio of the SDU brine (~22) reflects a system dominated by low-temperature solute inputs with a smaller but significant contribution from higher-temperature geothermal sources, consistent with the basin's paleohydrologic evolution.

3.2.3. *The Laguna Colorada and alkaline brines*

Alkaline brines represent a distinct geochemical regime in which Mg/Li ratios may no longer directly reflect the temperature of water-rock interactions of the inflow waters because Mg can be selectively removed from solution through the precipitation of Mg-silicates under elevated pH conditions. The following examples illustrate this process.

The third example is Laguna Colorada, a small (~52 km^2)(Risacher and Fritz, 1991a), moderately alkaline (pH ~8.0–8.4) saline lake located within the APMB that hosts active geothermal activity as well as several low-temperature springs and streams (Risacher and Fritz, 1991a; Scandiffio and Alvarez, 1990). The Mg/Li ratio of the lake brine is ~4. Risacher and Fritz (1991a) presented an evaporative transect of a representative inflow water to the lake. During the early stages of evaporation, Mg-silicates actively precipitate as pH increases to values as high as ~9.1 (Risacher and Fritz, 1991a). However, oxidation of aeolian sulfides and sulfur subsequently reverses the alkaline evaporative pathway of Hardie and Eugster (1970), forcing a decrease in pH to ~8.4 and inhibiting further Mg-silicate formation (Risacher and Fritz, 1991a).

During this process, Li behaves conservatively and does not appear to be significantly attenuated by water-sediment interactions (Risacher and Fritz, 1991a). As a result, the Mg/Li ratio of the evaporative transect decreases from ~8 to ~4 due to the selective removal of Mg into Mg-silicates (Fig. 3C); this equates to a roughly 50% removal of Mg assuming Li is conserved as suggested by Risacher and Fritz (1991a). Nonetheless, the overall magnitude of the Mg/Li ratio of the inflow waters is broadly preserved in the residual brine. This preservation is attributed to the reversal of the alkaline pathway, which limits extensive Mg-silicate precipitation, as reflected by the moderately alkaline pH of the lake brine. Given that Mg/Li ratios characteristic of high-temperature water-rock interactions range from ~16 to 0.4, both the inflow water (~8) and the lake brine (~4) are consistent with a dominant high-temperature contribution despite the partial, but significant, Mg removal.

Reversal of the alkaline evaporative pathway is a common feature of dilute inflow waters throughout the Lithium Triangle (Risacher et al., 2003; Risacher and Fritz, 2009; Risacher and Fritz, 1991a). These waters often originate from alteration of volcanic rocks that would otherwise promote an alkaline evolution. However the alkalinity reversal is induced by aeolian sulfide and sulfur oxidation, which is thought to be a primary reason why strongly alkaline brines are rare in the Lithium Triangle (Risacher et al., 2003; Risacher and Fritz, 2009; Risacher and Fritz, 1991a). Accordingly, the Laguna Colorada example demonstrates that such reversal processes can allow Mg/Li ratios of the brines to remain broadly representative of inflow conditions as waters evolve into brines, even in the presence of limited Mg-silicate formation.

Only a few strongly alkaline brines exist in the Lithium Triangle, and where the alkaline pathway reversal does not occur, Mg-silicate precipitation can exert a dominant control on Mg/Li ratios (Risacher and Fritz, 2009, Risacher and Fritz, 1991a). At Laguna Cachi (pH ~10) (Fig. 1), for example, inflow waters exhibit Mg/Li ratios between ~9 and 31, whereas the lake brine has a Mg/Li ratio of ~0.003, indicating extensive selective removal of Mg into Mg-silicates (Risacher and Fritz, 1991a); this equates to >99% removal of Mg assuming that Li is conserved in this system as it is in Laguna Colorada. Similar contrasts between inflows and brines are observed at other alkaline lakes with pH >9, including Lagunas Kara, Honda Sur, Catalcito, and Pelada in Bolivia. In these systems, Mg/Li ratios of the brines are controlled primarily by secondary mineral precipitation rather than the geochemical characteristics of the inflow waters, and therefore, fall outside the scope of the Mg/Li-temperature framework developed in this study. Consequently, Mg/Li ratios of brines should be interpreted in conjunction with pH and mineralogical context when assessing the thermal history of source waters to closed-basin brines. Notably, these alkaline brines display some of the lowest Mg/Li ratios reported in the Lithium Triangle, in stark contrast to the high Mg/Li ratios typically associated with low-temperature water-rock interactions in circumneutral pH brine systems.

3.2.4. The acid brines, the Salar de Gorbea & Salar Ignorado

Only two acid brines (pH ~1–3) are known to exist in the Lithium Triangle; the adjacent closed basins of the Salar de Gorbea and Salar Ignorado in Chile (Fig. 1B) (Pueyo et al., 2021; Risacher et al., 2002). Importantly, the chemistries of these brines are unique and their formation is distinct from any other brine system in the Lithium Triangle (Risacher et al., 2002). Despite this, they both formed from the same interplay of high- and low-temperature water-rock interactions that, as shown in this study, govern the Mg/Li ratio in other brines.

These brines arise from nearby volcanic rocks are the remnants of an intensely hydrothermally altered volcanic core (Cornejo, 1987; Risacher et al., 2002). As a result (1) the natural buffering capacity of the volcanic rocks have been greatly diminished; and (2) primary minerals of the volcanic rocks have been almost completely replaced or altered to secondary minerals including chlorite and elemental sulfur (Cornejo, 1987; Risacher et al., 2002). Oxidation of the elemental sulfur provides the necessary acidity that cannot be neutralized by the altered volcanic rock, allowing the formation of acid brines (Risacher et al., 2002). Today, geothermal waters do not occur in the basin (Risacher et al., 2002) and the salt flats are primarily fed by near-surface waters interacting with the intensely altered rocks that evaporate to form the salar brines (Pueyo et al., 2021; Risacher et al., 2002). Nevertheless, there is evidence from fluid inclusions and sulfur and oxygen isotopes in gypsum to support several periods of historic geothermal activity and inputs to the salars (Karmanocky III and Benison, 2016; Pueyo et al., 2021).

As mentioned in earlier discussion of geothermal systems, higher-temperature water-rock interactions lead to greater incorporation of Mg into secondary mineral phases, while Li remains in solution, resulting in conspicuously low Mg/Li in geothermal waters. This would seem to be apparent in the hydrothermally altered rocks surrounding the Salar de Gorbea and Salar Ignorado as chlorite, a common Mg-rich secondary mineral in hydrothermal systems, has a major occurrence (Cornejo, 1987; Risacher et al., 2002). This deposition of Mg-rich secondary minerals has presumably increased the Mg/Li ratio of the altered volcanic rocks from their original values, however this data is not available. Despite this, we know that the Mg/Li ratio in the brines of these two salars are some of the highest at ~88 for the Salar de Gorbea and ~ 316 for Salar Ignorado (medians from the compiled dataset). While the two salars are very similar in terms of geology and geochemistry, the generally higher salinity and presence of Mg-sulfate minerals at Gorbea and their absence at Ignorado (Benison, 2019) could explain the relatively lower Mg/Li ratio at Gorbea if all else is equal. We posit that the relatively high Mg/Li ratios in these brines are linked to the high-temperature hydrothermal alteration of the nearby volcanic rocks and the replacement of primary minerals with Mg-rich secondary mineral phases. Since near surface processes control water and solute inputs to the salar brines in the modern day, it seems likely that relatively low-temperature water-rock interactions with the rocks that were previously modified by high-temperature hydrothermal alteration have produced the distinctly elevated Mg/Li ratios we see in the brines from these basins today. In this sense, the Mg/Li ratios of the Gorbea and Ignorado brines reflect an inherited geochemical signature imposed by earlier high-temperature hydrothermal alteration, rather than contemporary geothermal fluid inputs that would otherwise contribute a much lower Mg/Li ratio. These acid brines therefore demonstrate that the Mg/Li ratios of brines are closely linked to source rock composition and record the thermal history of water-rock interactions, further emphasizing the importance of inherited geochemical signatures in closed-basin brine systems.

4. An overview of Mg/Li ratios in closed-basin brines

4.1. Extrapolating observed trends across the Lithium Triangle

The results presented in this study define a coherent framework for interpreting Mg/Li ratios in closed-basin brines across the Lithium Triangle. At the scale of individual inflows, Mg/Li ratios are primarily established by the temperature of water-rock interactions, with high-temperature interactions producing low Mg/Li ratios, while low-temperature, near-surface interactions producing relatively high ratios that resemble those of source rocks (Fig. 2). This concept follows well known trends in geothermal systems and is supported by experimental results (Kharaka and Mariner, 1989; Yuan et al., 2021).

At the basin scale, Mg/Li ratios in brines reflect the integration of these source signatures through mixing of multiple inflows with distinct thermal histories. The case studies presented in this study demonstrate that closed-basin brines are often not derived from a single solute source; instead, their Mg/Li ratios represent mixing-weighted composites of geothermal and near-surface water inputs. While subsequent evaporative concentration and mineral precipitation govern absolute solute concentrations, they generally exert a relatively minor influence on Mg/Li ratios under the predominantly circumneutral pH conditions that characterize most Lithium Triangle brines.

Across the Lithium Triangle, brines consistently form through similar evaporative evolutionary pathways that typically result in circumneutral Na-Cl-(SO_4) brines (López Steinmetz and Salvi, 2021; Risacher and Fritz, 2009; Williams et al., 2025a), occasionally with Ca or Mg enrichments (Lowenstein and Risacher, 2009; Risacher et al., 2003; Risacher and Fritz, 2009). This evolution may occur either through direct evaporation of inflowing waters or through reversal of an initially alkaline evaporative pathway induced by oxidation of aeolian sulfur and sulfides, as documented for Laguna Colorada (Lowenstein and Risacher, 2009; Risacher and Fritz, 1991a). The dilute waters required to initially follow an alkaline pathway generally derive from near-surface alteration of local volcanic rocks and are not typically considered a dominant source of solutes to closed basins (Risacher and Fritz, 2009; Risacher and Fritz, 1991a). In contrast, brackish inflows, often generated in part through recycling of pre-existing closed-basin brines, are thought to represent the primary source of solutes to many basins of the Lithium Triangle (Risacher and Fritz, 2009; Risacher and Fritz, 1991a).

Regardless of inflow composition, evaporative evolution leads to precipitation of a broadly similar suite of minerals in the majority of the basins, including calcite, gypsum, ulexite, and halite (Lowenstein and Risacher, 2009; Williams et al., 2026). As demonstrated in the case studies presented in this paper (e.g., LPG), precipitation of these phases does not significantly modify Mg/Li ratios under circumneutral pH conditions. Mg/Li ratios are only substantially altered when Mg-silicates form under alkaline conditions, as observed in Laguna Colorada and Laguna Cachi. The widespread similarity in brine chemistries across the Lithium Triangle therefore implies that common mechanisms control

brine formation and supports the broader applicability of the framework presented in this study. This does not imply that all systems behave identically; for example, the Salar de Atacama does not host an alkaline brine, yet minor microbially mediated Mg-silicate precipitation has been documented in pools around the salar margin (Suosaari et al., 2026). Although not addressed explicitly in this study, such microbial processes may play an additional role in modulating Mg or Li concentrations and has been documented in other salars (Suosaari et al., 2022a, 2022b). Accordingly, this warrants further investigation.

Considering the role of water-sediment interactions, our results show that both Mg and Li can be significantly retained in sediments even in the absence of primary Mg- or Li-bearing mineral precipitation (e.g., the Rio Grande Delta). The extent of such water-sediment interaction varies among closed basins, as not all systems possess large deltaic environments (e.g., LPG) where sediment interaction is pronounced. This variability is reflected in the wide range of δ^7Li values observed in Lithium Triangle brines, spanning approximately ~3‰ to 16‰ (Desaulty et al., 2022; Meixner et al., 2022), with higher values generally indicating more extensive water-sediment interaction and Li retention. While not investigated here further research is necessary to determine and quantify the mechanisms of attenuation to sediments (i.e., adsorption, incorporation into detrital or evaporative minerals, etc.), perhaps by integrating both Mg and Li isotope systematics.

Despite this variability, observations from both LPG and the Rio Grande Delta demonstrate that the magnitude of the Mg/Li ratio of the inflows is largely preserved, even when substantial fractions of Mg and Li are both removed from solution during water-sediment interaction. This preservation likely reflects broadly similar attenuation efficiencies of Mg and Li under these conditions as demonstrated for the Rio Gande delta at the SDU. In addition, many closed-basin brines are not derived from a single inflow source but instead receive multiple inflows with distinct thermal histories.

The Salar de Atacama provides a further example of such mixing, as it is a large salt flat receiving waters from multiple sources, including possible geothermal inputs from the nearby El Tatio geothermal system (Godfrey and Álvarez-Amado, 2020; Lowenstein and Risacher, 2009). The Mg/Li ratio of the Salar de Atacama therefore likely reflects a mixture of high- and low-temperature water-rock interaction signatures. Its relatively low Mg/Li ratio (~7–8) (López Steinmetz and Salvi, 2021; the compiled dataset), however, suggests a greater proportional contribution from geothermal sources compared to the SDU (Mg/Li ≈ 22). This interpretation is consistent with the paleohydrologic evolution of the SDU, which incorporates solutes from paleolake-derived brines that integrated inputs across the Altiplano, including substantial surficial water contributions associated with low-temperature water-rock interactions.

4.2. Distribution of Mg/Li ratio in brines across the Lithium Triangle

We compiled data for 103 closed basins of the Lithium Triangle across Chile ($n = 52$), Bolivia ($n = 33$), and Argentina ($n = 18$), including basins hosting freshwater lakes, saline lakes, and hypersaline brines in salar and playa environments. Of these basins, 80 contain brines with TDS greater than 35 g/L (approximately that of seawater), and 91 are not considered alkaline (i.e., median pH < 9). Median Mg/Li ratios vary widely among basins, ranging from 0.003 (Laguna Cachi, Bolivia) to 722 (Salar de Michincha, Chile).

To facilitate regional comparison, Mg/Li ratios were grouped into broad ranges indicative of fluids with different dominant thermal influences, recognizing that these categories reflect integrated Mg/Li signatures rather than discrete water sources with specific water-rock interaction temperatures. Importantly, this classification does not capture the specific processes, such as mixing between endmembers that produced a given Mg/Li ratio, and such interpretations must be made on a basin-by-basin basis. Nonetheless, within this framework and only considering brines with a circumneutral pH, 57 closed-basin brines and waters have median Mg/Li ratios that fall within ranges indicative of inflows of high-temperature influence ($16 > Mg/Li \geq 0.4$); 21 fall within ranges indicative of inflows with moderate-temperature influence ($68 > Mg/Li \geq 16$); and 12 exhibit Mg/Li ratios ≥68, consistent with a dominant near-surface water inflow with a low-temperature water-rock interaction fingerprint. Values lower than 0.4 occur only in three alkaline brines where Mg-silicate precipitation is inferred to strongly modify Mg/Li ratios; as such, no basins are interpreted as reflecting inflows originating from a very-high-temperature source on the basis of Mg/Li alone. Table A1 summarizes Mg/Li ratios of closed-basin brines and waters from across the Lithium Triangle and their inferred dominant thermal regimes of the inflow waters. Fig. 1B illustrates the spatial distribution of Mg/Li ratios across the Lithium Triangle.

Although very-high-temperature (>200 °C) geothermal systems are known to exist in the Lithium Triangle (Giggenbach, 1978; Munoz-Saez et al., 2018), the absence of extremely low Mg/Li ratios in most brines does not imply that such geothermal fluids fail to contribute solutes to closed basins. Rather, this pattern suggests that mixing with waters derived from lower-temperature water-rock interactions occurs in essentially all systems, and therefore, geothermal fluids are rarely the sole source of solutes that flow into the salar systems. As demonstrated by the SDU and Rio Grande case studies, Mg/Li ratios in brines are best interpreted as mixing-weighted composites of multiple inflows with distinct thermal histories. Consequently, brines with Mg/Li ratios falling within ranges indicative of high- or moderate-temperature influence likely reflect varying proportions of high- and low-temperature inputs rather than exclusive derivation from a single thermal regime.

Previous studies have noted the absence of clear geographic trends in Mg/Li ratios across the Lithium Triangle (López Steinmetz and Salvi, 2021). Nevertheless, several qualitative spatial associations emerge when Mg/Li ratios are considered alongside regional geology. Nearly all brines in Argentina exhibit relatively low Mg/Li ratios consistent with a dominant high-temperature influence (Fig. 1B; Table A1), potentially reflecting the fact that most Argentine closed basins lie within or adjacent to the APMB or SPMB, where geothermal activity is widespread (Cortes-Calderon et al., 2025; Peralta Arnold et al., 2017; Reinoso Carbonell et al., 2025). A similar pattern is observed among small closed-basin brines of the high Altiplano-Puna region of Chile, east of the Salar de Atacama, which form two groups: basins located within the APMB that generally exhibit Mg/Li ratios <10, and basins just south of the APMB with Mg/Li ratios >50 (Fig. 1B). This contrast suggests the possible impact of more direct geothermal influence within the APMB and diminished contributions of geothermal inputs in basins further south.

The Mg/Li spatial association does not hold uniformly across the southern Bolivian Altiplano (i.e., Sud Lípez), where numerous closed basins situated within the APMB display a wide range of Mg/Li ratios, from <0.4 in alkaline brines affected by Mg-silicate precipitation to values >68 indicative of low-temperature inflows (Fig. 1B). This variability may reflect the generally reduced geothermal discharge at the surface in this area relative to northern Chile (Scandiffio and Alvarez, 1990), allowing near-surface, low-temperature water-rock interactions to dominate solute inputs in some basins. The presence of alkaline lakes and brines in this region, systems that likely formed from evaporation of waters derived from volcanic rock alteration rather than geothermal fluids, further supports this interpretation (Risacher and Fritz, 2009; Risacher and Fritz, 1991a).

4.3. Brine types and the relative enrichment of Mg

Most closed-basin brines of the Lithium Triangle are of the Na-Cl-(SO_4) type according to the classification scheme of Eugster and Hardie (1978), with occasional enrichments of Mg or Ca (López Steinmetz and Salvi, 2021; Lowenstein and Risacher, 2009; Risacher and Fritz, 2009; Williams et al., 2026; Williams et al., 2025a). In nearly all cases, Na remains the dominant cation unless extreme evaporation and halite

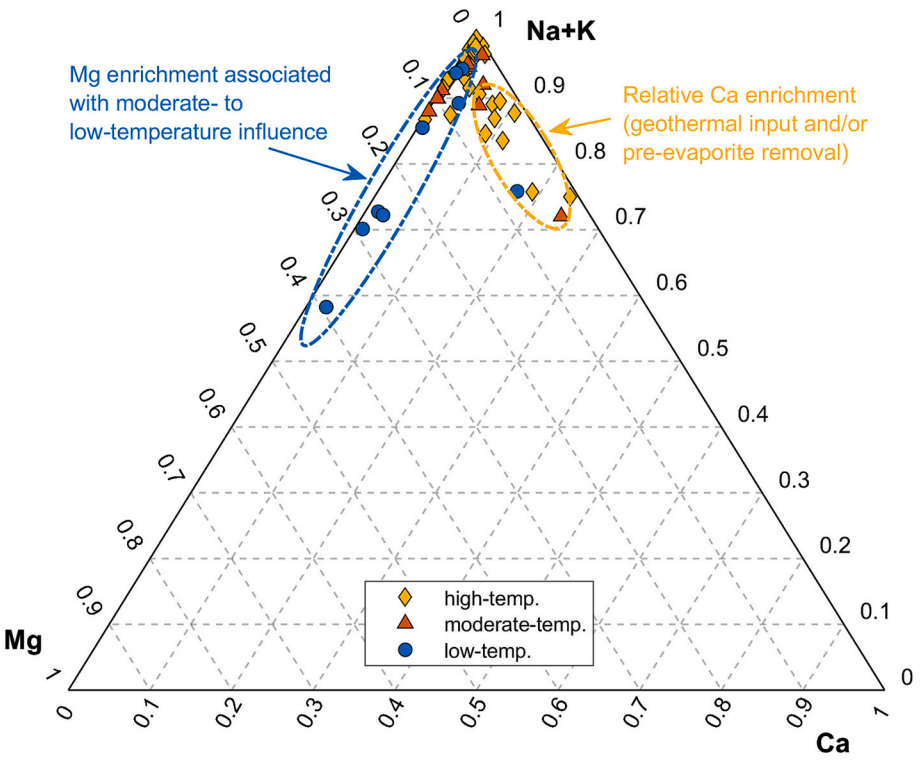

Fig. 5. Ternary diagram of major cation compositions (Na+K, Mg, Ca; relative mol%) for closed-basin brines of the Lithium Triangle, using median values for each basin (TDS > 50 g/L). Na (+K) is the dominant cation in nearly all systems. Relative Mg enrichment is mostly observed in brines whose Mg/Li ratios indicate dominant low- to moderate-temperature influence, whereas relative Ca enrichment occurs primarily in brines classified as high-temperature influenced or in comparatively low-salinity systems prior to extensive Ca removal through evaporite precipitation. Alkaline and acid brines not shown. All data from the compiled dataset.

precipitation substantially modify brine chemistry (Williams et al., 2026). Calcium concentrations are broadly governed by the precipitation of calcite, ulexite, and gypsum, (Risacher and Fritz, 2009; Williams et al., 2026) although relative Ca enrichment may also reflect geothermal inputs (Lowenstein and Risacher, 2009).

Magnesium, in contrast, can locally become a major cation (>5 mol % of cations). In classical evaporative systems, Mg enrichment is commonly associated with waters interacting with more mafic lithologies that are inherently Mg-rich (Eugster and Hardie, 1978; Hardie and Eugster, 1970). However, the origin of Mg enrichment in Lithium Triangle brines has not been systematically evaluated in the context of temperature-dependent water-rock interaction.

To examine this relationship, we plot median major-cation compositions (Na+K, Mg, Ca) of closed basins with TDS > 50 g/L on a standard

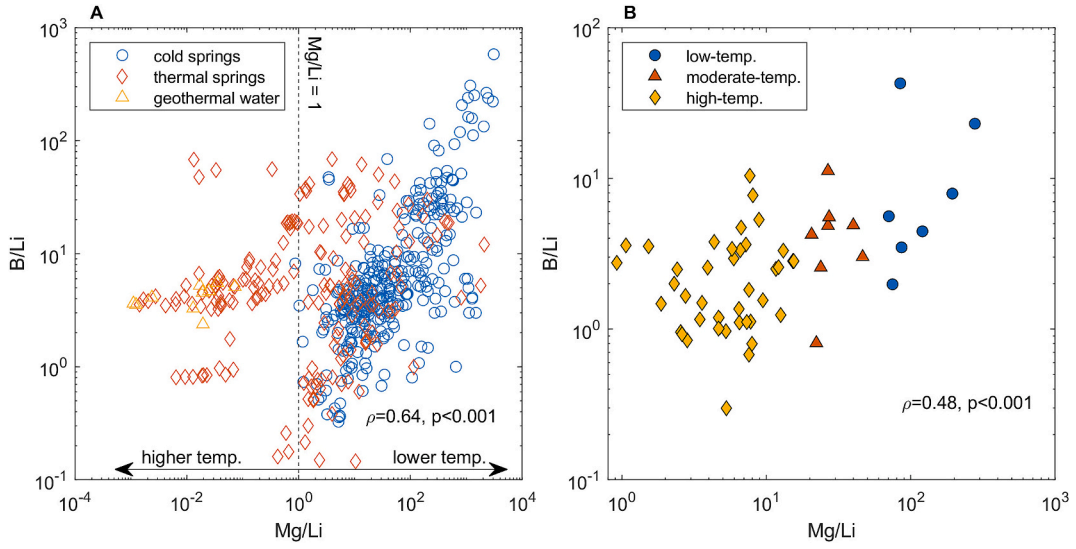

Fig. 6. (A) Co-variation of Mg/Li and B/Li (mass ratios) in spring waters across the Lithium Triangle. This suggests that the relative enrichment of B and Li is temperature dependent much like Mg/Li is and that low-temperature water-rock interactions lead to higher B/Li ratios. (B) Median Mg/Li and B/Li ratios in closed-basin brines of the Lithium Triangle with TDS > 50 g/L. A similar positive correlation exists in the brines suggesting that the same controls on the Mg/Li ratio also apply for B enrichment relative to Li. Alkaline and acid brines not shown. All data from the compiled dataset.

ternary diagram and distinguish them according to the Mg/Li thermal classification developed above (Fig. 5). Two primary patterns emerge. First, brines with relative Mg enrichment are predominantly classified within the low- to moderate-temperature influence fields (Fig. 5), consistent with enhanced Mg contributions from low-temperature near-surface water-rock interaction or mixed inflows. Second, relative Ca enrichment is observed either in comparatively low-salinity systems (prior to substantial Ca removal through evaporite precipitation) or in brines classified as high-temperature influenced, consistent with geothermal Ca inputs (Fig. 5).

These relationships suggest that major-cation systematics broadly support the Mg/Li-based thermal framework: Mg enrichment tends to accompany systems dominated by lower-temperature water-rock interaction, whereas Ca enrichment more commonly reflects either early evaporative stages or geothermal influence. Although major-cation compositions are modified by evaporative processes, their distribution provides an independent line of evidence linking brine chemistry to the integrated thermal history of solute sources as inferred by the distribution of Mg/Li ratios.

4.4. Links between the relative enrichment of B, Mg, and Li

While this study primarily focuses on the use of Mg/Li to delineate between dominantly high- and low-temperature water-rock interactions of the inflow waters and how this can lead to differential enrichment of Mg and Li in brines, the relative enrichment of boron (B) over Li has also long been a topic of interest in studies of closed-basin brines (López Steinmetz and Salvi, 2021; Risacher, 1984). Across spring waters of the Lithium Triangle (both thermal and cold) we show a strong positive correlation between Mg/Li and B/Li ratios, whereas at Mg/Li ratios below ~1, B/Li ratios become comparatively invariant (Fig. 6A). These relationships suggest a potential coupling between the processes that control Mg/Li and those governing B/Li during water-rock interactions.

One possible interpretation is that the differential enrichment of B and Li in spring waters may also depend on the temperature of water-rock interactions, with higher B/Li ratios associated with higher Mg/Li ratios and therefore with lower-temperature water-rock interaction conditions. Conversely, the apparent invariance of B/Li at low Mg/Li ratios (<1), which are characteristic of high-temperature systems, suggests that different processes may control B behavior under these high-temperature conditions. For example, secondary mineral formation in high-temperature environments, including clays and chlorite, can both sequester and release B and Li, potentially fractionating B/Li ratios (Reyes and Trompetter, 2012; Schmidt et al., 2025).

Consistent with this interpretation, the SDU and SDC, both characterized by Mg/Li ratios indicative of moderate-temperature influence and mixed solute origins, are also known to exhibit pronounced co-enrichment of B over Li (e.g., B/Li ~ 3.0 at the SDC) relative to many other closed-basin brines in the Lithium Triangle (e.g., B/Li ~0.8 at the Salar de Atacama) (Risacher, 1984; Risacher and Fritz, 1991b). A comparison of median Mg/Li and B/Li ratios for closed-basin brines with median TDS values greater than 50 g/L reveals a clear positive relationship, with brines exhibiting high Mg/Li ratios consistent with dominant low-temperature influence also displaying the highest B/Li ratios (Fig. 6B). Table A1 also compiles the median B/Li ratio for each closed-basin brine relative to the inferred water-rock interaction temperature.

These observations suggest that low-temperature water-rock interactions may play an important role in promoting high B co-enrichment with Li in some closed-basin brines. However, this interpretation remains tentative since B is not conservative during evaporative evolution due to the precipitation of borate minerals (typically ulexite) that are found in nearly every salar system of the Lithium Triangle, directly modifying B/Li ratios of residual brines (Alonso and Viramonte, 1990; Orris, 1995; Williams et al., 2026). Regardless, the clear correlations between Mg/Li and B/Li in spring waters and closed-basin brines demonstrate that the temperature of water-rock interactions that control the composition of inflow waters may be an important process in controlling the relative enrichment of B over Li also in the brines of the Lithium Triangle. Further work is necessary to confirm these relationships and to link variations in the B/Li ratios of inflow waters to the values in local volcanic rocks and their alteration.

5. Conclusion

This study utilizes Mg/Li ratios of spring waters and closed-basin

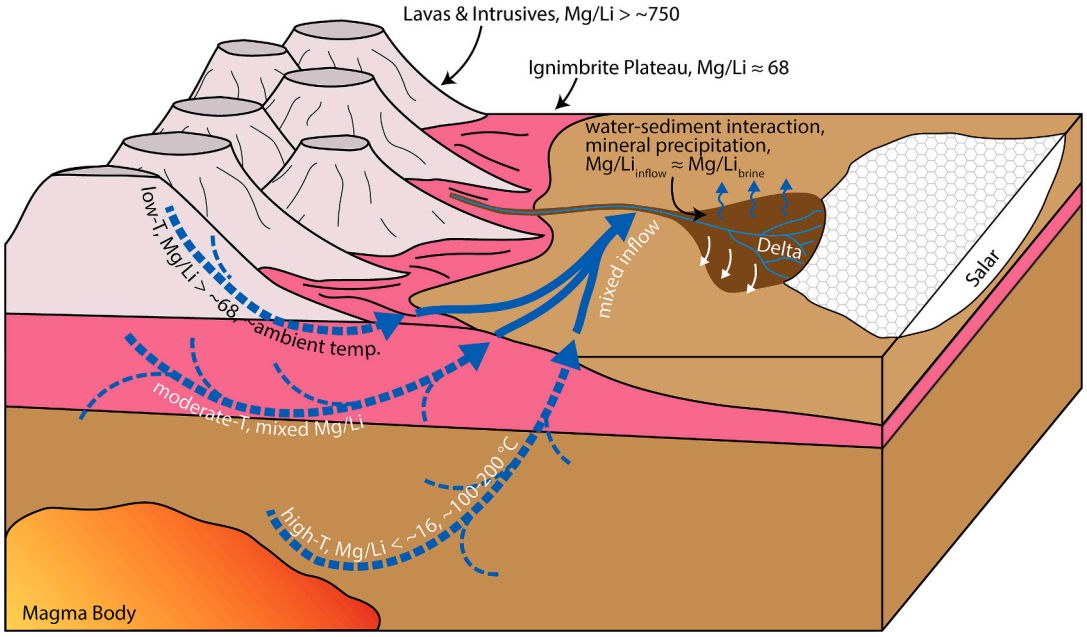

Fig. 7. Schematic diagram illustrating the major controls on Mg/Li ratios in closed-basin brines of the Lithium Triangle: (1) temperature-dependent water-rock interactions establish initial source Mg/Li signatures in waters; (2) mixing integrates these signatures at the basin scale; and (3) evaporative and sedimentary processes generally preserve the integrated Mg/Li ratio under circumneutral conditions. This does not cover variations relevant to alkaline brines.

brines as a geochemical tool to elucidate the relative roles of high- and low-temperature water-rock interactions of the water sources that supply solutes to closed basins of the Lithium Triangle. In geothermal systems, Mg is preferentially incorporated into secondary mineral phases relative to Li, resulting in distinctive low Mg/Li ratios, whereas under low-temperature, near-surface conditions, aqueous Mg/Li ratios closely resemble those of local source rocks and are therefore relatively high. These temperature-dependent processes establish the initial Mg/Li signatures of dilute inflow waters that flow into the closed basins (Fig. 7).

As waters evolve towards closed-basin brines, several additional processes can modify the Mg/Li ratios, including mixing of multiple water sources, evaporative concentration and mineral precipitation, and attenuation of Mg and Li during water-sediment interactions. Our results demonstrate that, aside from mixing between inflows with distinct thermal histories, these processes generally exert only a limited influence on the magnitude of Mg/Li ratios during brine evolution. This preservation is largely attributable to the circumneutral pH that controls the geochemical evolution of most Lithium Triangle brines, which inhibits extensive precipitation of Mg-silicates (and/or Mg-carbonates). Although both Mg and Li can be scavenged during water-sediment interactions, their similar removal efficiencies appear to result in minimal fractionation of the Mg/Li ratio during the evolution of inflow waters to become closed-basin brines.

Consequently, the Mg/Li ratio of closed-basin brines in the Lithium Triangle reflects the integrated thermal history of inflow sources, with basin-scale mixing between high- and low-temperature inputs acting as the primary modulator of the final brine composition. This is broadly summarized in Fig. 7. When interpreted alongside pH, basin hydrology, and evidence for mixing, Mg/Li ratios provide a simple yet powerful and robust tool for distinguishing between geothermal-dominated and near-surface-dominated solute inputs in closed-basin brine systems. Future work integrating Mg/Li ratios with isotopic tracers, basin-scale hydrologic models, and sediment mineralogy will help further constrain the magnitude of high- and low-temperature solute inputs.

Beyond the Lithium Triangle, Li-rich brines primarily occur in closed basins of the Tibetan Plateau and the western United States, many of which exhibit similar Na-Cl-(SO_4) chemical composition, have circumneutral pH, and are spatially associated with active geothermal systems (Munk et al., 2025; Williams et al., 2025a; Zheng and Liu, 2009). These similarities suggest that the framework developed in this study may be broadly applicable to other continental brine systems, although further work is needed to evaluate regional differences in Mg and Li cycling and sedimentary modification processes.

Declaration of competing interest

The authors declare that they have no known competing financial interests or personal relationships that could have appeared to influence the work reported in this paper.

Acknowledgments

The authors would like to thank K. Ledebur (Andean Information Network) who provided invaluable logistical and field support and Y. Cruz (FRUTCAS) and R. Calizaya who provided substantial insight and support during the sampling campaigns. This study was supported by the Duke University Climate Research Innovation Seed Program, CRISP and the Duke University Josiah Charles Trent Memorial Foundation Endowment Fund. G.D.Z.W. benefitted from the Duke University Graduate Student International Dissertation Research Travel Fellowship. The authors would also like to thank R.C. Hill, H. Wudke, G.A. Hall, and G.S. Dwyer from Duke for help with analytical and field tasks and data curation. We also thank two anonymous reviewers for their thorough and detailed reviews, which have improved the quality of this paper.

Appendix A

Table A1
Median Mg/Li mass ratios, B/Li mass ratios, and pH values for closed-basin brines of the Lithium Triangle based on the compiled dataset, with the inferred dominant water-rock interaction regimes. Classifications reflect integrated Mg/Li signatures resulting from mixing of solute sources with different thermal histories and do not imply a single water-rock interaction temperature. The name of salars/basins generally follow those used by Risacher et al. (1999) for Chilean salars/basins, Risacher and Fritz (1991a, 1991b) for Bolivian salars/basins, and López Steinmetz and Salvi (2021) for Argentine salars/basins.

Basin	Country	Samples (n=)	Mg/Li (median)	B/Li (median)	pH (median)	Dominant Water-Rock Interaction Regime
Antofalla-Botijuelas	Argentina	6	4.1	5.9	7.6	high-temp. influenced
Laguna de Guayatayoc	Argentina	3	1.1	3.6	7.6	high-temp. influenced
Laguna del Peinado	Argentina	7	9.5	1.4	7.9	high-temp. influenced
Salar de Arizaro	Argentina	12	7.7	10	7.4	high-temp. influenced
Salar de Cauchari	Argentina	5	2.4	2.5	8.6	high-temp. influenced
Salar de Centenario	Argentina	5	11	4.4	7.6	high-temp. influenced
Salar de Diablillos	Argentina	4	8.9	5.3	8.0	high-temp. influenced
Salar de Incahuasi	Argentina	5	120	4.4	6.9	low-temp. influenced
Salar de Jama	Argentina	10	21	95	8.2	moderate-temp./mixed-origin
Salar de Olaroz	Argentina	34	2.3	2.0	7.2	high-temp. influenced
Salar de Pastos Grandes	Argentina	309	6.5	1.4	6.8	high-temp. influenced
Salar de Pocitos-Quirón	Argentina	10	9.4	2.3	7.9	high-temp. influenced
Salar de Pozuelos	Argentina	20	5.3	1.0	8.1	high-temp. influenced
Salar de Ratones	Argentina	3	1.5	3.5	7.5	high-temp. influenced
Salar de Rincón	Argentina	10	8.1	7.7	8.8	high-temp. influenced
Salar de Río Grande	Argentina	10	4.7	1.0	7.1	high-temp. influenced
Salar del Hombre Muerto	Argentina	10	1.9	1.5	7.8	high-temp. influenced
Salinas Grande	Argentina	10	3.6	1.5	7.5	high-temp. influenced
Laguna Balivian	Bolivia	1	21	4.2	7.1	moderate-temp./mixed-origin
Laguna Bush	Bolivia	1	0.9	2.8	8.3	high-temp. influenced
Laguna Cachi	Bolivia	1	0.003	2.9	10.1	N/A, alkaline
Laguna Canapa	Bolivia	1	2.8	1.7	7.8	high-temp. influenced
Laguna Capina	Bolivia	1	1.3	1.4	8.6	high-temp. influenced

(continued on next page)

Table A1 (*continued*)

Basin	Country	Samples (n=)	Mg/Li (median)	B/Li (median)	pH (median)	Dominant Water-Rock Interaction Regime
Laguna Catalcito	Bolivia	1	0.3	1.7	9.1	N/A, alkaline
Laguna Chiar Kota	Bolivia	1	6.5	1.1	7.4	high-temp. influenced
Laguna Chohillas	Bolivia	1	2.9	1.6	7.6	high-temp. influenced
Laguna Chulluncani	Bolivia	1	85	43	8.8	low-temp. influenced
Laguna Collpa	Bolivia	1	5.4	163	10.8	N/A, alkaline
Laguna Colorada	Bolivia	2	4.4	3.8	8.2	high-temp. influenced
Laguna Coruto	Bolivia	1	4.7	1.2	7.8	high-temp. influenced
Laguna Hediona	Bolivia	1	9.4	1.6	6.7	high-temp. influenced
Laguna Hedionia Sur	Bolivia	1	13	227	10.6	N/A, alkaline
Laguna Honda	Bolivia	1	2.4	1.5	7.9	high-temp. influenced
Laguna Honda Sur	Bolivia	1	0.006	3.2	9.5	N/A, alkaline
Laguna Kara	Bolivia	1	1.8	2.4	9.4	N/A, alkaline
Laguna Loromayu	Bolivia	1	2.8	0.8	7.8	high-temp. influenced
Laguna Luriques	Bolivia	1	1.2	0.9	8.9	high-temp. influenced
Laguna Mahama Coma	Bolivia	1	13	1.2	7.4	high-temp. influenced
Laguna Pastos Grandes	Bolivia	11	2.6	1.0	7.5	high-temp. influenced
Laguna Pelada	Bolivia	1	4.1	16	9.1	N/A, alkaline
Laguna Pujio	Bolivia	1	6.7	4.7	7.6	high-temp. influenced
Laguna Puripica	Bolivia	1	2.5	2.2	8.5	high-temp. influenced
Laguna Ramaditas	Bolivia	1	27	5.5	7.1	moderate-temp./mixed-origin
Laguna Totoral	Bolivia	1	2.5	4.9	10.3	N/A, alkaline
Laguna Turquiri	Bolivia	1	39	15	8.3	moderate-temp./mixed-origin
Laguna Verde	Bolivia	1	7.2	3.6	8.5	high-temp. influenced
Lagunillas	Bolivia	1	262	299	9.8	N/A, alkaline
Salar de Chalviri	Bolivia	2	35	15	8.3	moderate-temp./mixed-origin
Salar de Coipasa	Bolivia	14	46	3.0	7.4	moderate-temp./mixed-origin
Salar de Empexa	Bolivia	4	32	1.0	7.0	moderate-temp./mixed-origin
Salar de Uyuni	Bolivia	249	22	0.8	6.9	moderate-temp./mixed-origin
Lago Chungara	Chile	3	363	3.3	9.2	N/A, alkaline
Laguna Chivato Muerto	Chile	1	27	4.8	8.7	moderate-temp./mixed-origin
Laguna Escondida	Chile	4	166	20	8.6	low-temp. influenced
Laguna Helada	Chile	1	3.5	1.2	7.5	high-temp. influenced
Laguna Lagunilla	Chile	1	137	15	8.9	low-temp. influenced
Laguna Lejia	Chile	1	194	7.9	8.2	low-temp. influenced
Laguna Minique	Chile	3	143	24	8.5	low-temp. influenced
Laguna Miscanti	Chile	2	90	21	8.5	low-temp. influenced
Laguna Trinchera	Chile	1	8.5	3.7	7.5	high-temp. influenced
Laguna Tuyajito	Chile	2	75	2.0	7.6	low-temp. influenced
Laguna Verde	Chile	3	12	2.1	8.1	high-temp. influenced
Laguna de la Azufrera	Chile	1	278	23	7.6	low-temp. influenced
Laguna del Bayo	Chile	1	15	8.2	8.6	high-temp. influenced
Laguna del Negro Franscisco	Chile	2	15	2.8	8.0	high-temp. influenced
Lagunas Bravas	Chile	2	6.6	3.3	8.5	high-temp. influenced
Lagunas Cotacotani	Chile	3	321	3.5	9.2	N/A, alkaline
Lagunas del Jilguero	Chile	4	12	5.6	8.5	high-temp. influenced
Salar Grande	Chile	2	13	3.3	6.7	high-temp. influenced
Salar Ignorado	Chile	2	316	11	3.1	N/A, acid
Salar de Agua Amarga	Chile	4	24	2.6	7.5	moderate-temp./mixed-origin
Salar de Aguas Calientes 1	Chile	2	3.9	2.6	7.4	high-temp. influenced
Salar de Aguas Calientes 2	Chile	2	55	3.8	7.8	moderate-temp./mixed-origin
Salar de Aguas Calientes 3	Chile	2	60	3.9	8.5	moderate-temp./mixed-origin
Salar de Aguas Calientes 4	Chile	5	26	5.1	8.3	moderate-temp./mixed-origin
Salar de Aguilar	Chile	3	12	2.6	6.9	high-temp. influenced
Salar de Alconcha	Chile	1	27	11	8.7	moderate-temp./mixed-origin
Salar de Ascotan	Chile	16	10	3.5	8.2	high-temp. influenced
Salar de Atacama	Chile	88	7.9	0.8	6.9	high-temp. influenced
Salar de Capur	Chile	5	86	3.5	8.0	low-temp. influenced
Salar de Carcote	Chile	12	16	2.8	7.6	high-temp. influenced
Salar de Coposa	Chile	7	40	3.2	8.4	moderate-temp./mixed-origin
Salar de Gorbea	Chile	8	88	5.6	2.5	N/A, acid
Salar de Huasco	Chile	5	8.5	4.7	8.7	high-temp. influenced
Salar de Imilac	Chile	3	35	2.5	7.5	moderate-temp./mixed-origin
Salar de Infieles	Chile	4	19	2.9	7.8	moderate-temp./mixed-origin
Salar de Laco	Chile	2	36	2.4	8.1	moderate-temp./mixed-origin
Salar de Loyoques	Chile	1	7.6	1.8	6.6	high-temp. influenced
Salar de Maricunga	Chile	2	7.6	0.7	6.5	high-temp. influenced
Salar de Michincha	Chile	5	722	12	8.7	low-temp. influenced
Salar de Pajonales	Chile	8	40	4.9	7.5	moderate-temp./mixed-origin
Salar de Pedernales	Chile	5	7.8	1.1	7.5	high-temp. influenced
Salar de Pintados	Chile	8	11	2.9	8.1	high-temp. influenced
Salar de Pujsa	Chile	1	5.2	3.9	9.0	
Salar de Punta Negra	Chile	7	15	1.2	8.1	high-temp. influenced
Salar de Surire	Chile	11	5.6	3.3	8.0	high-temp. influenced
Salar de Tara	Chile	1	2.6	0.9	8.0	high-temp. influenced
Salar de Wheelwright	Chile	2	5.8	3.4	6.9	high-temp. influenced
Salar de la Azufrera	Chile	3	70	5.6	7.2	low-temp. influenced

(*continued on next page*)

Table A1 (*continued*)

Basin	Country	Samples (n=)	Mg/Li (median)	B/Li (median)	pH (median)	Dominant Water-Rock Interaction Regime
Salar de la Isla	Chile	9	5.3	0.3	7.3	high-temp. influenced
Salar de la Laguna	Chile	1	22	7.8	8.3	moderate-temp./mixed-origin
Salar de la Piedra Parada	Chile	7	24	3.6	8.3	moderate-temp./mixed-origin
Salar de las Parinas	Chile	5	7.3	1.1	7.6	high-temp. influenced

Appendix B. Supplementary data

Supplementary data to this article can be found online at https://doi.org/10.1016/j.earscirev.2026.105516.

Data availability

All data are available in the paper and supplement

References

Alam, M.A., Muñoz, A., 2024. A critical evaluation of the role of a geothermal system in lithium enrichment of brines in the salt flats: a case study from Laguna Verde in the Atacama region of Chile. Geothermics 119, 102970. https://doi.org/10.1016/j.geothermics.2024.102970.

Alonso, R.N., Viramonte, J.G., 1990. Borate deposits in the Andes. In: Fontboté, L., Amstutz, G.C., Cardozo, M., Cedillo, E., Frutos, J. (Eds.), Stratabound Ore Deposits in the Andes. Springer, Berlin, Heidelberg, pp. 721–732. https://doi.org/10.1007/978-3-642-88282-1_57.

Álvarez-Amado, F., Rosales, M., Godfrey, L., Poblete-González, C., Morgado, E., Espinoza, M., Hidalgo-Gajardo, A., Volosky, D., Cortés-Aranda, J., 2022a. The role of ignimbrites and fine sediments in the lithium distribution and isotopic fractionation in hyperarid environments: insights from li-isotopes in the Atacama desert. J. Geochem. Explor. 241, 107062. https://doi.org/10.1016/j.gexplo.2022.107062.

Álvarez-Amado, F., Tardani, D., Poblete-González, C., Godfrey, L., Matte-Estrada, D., 2022b. Hydrogeochemical processes controlling the water composition in a hyperarid environment: new insights from Li, B, and Sr isotopes in the Salar de atacama. Sci. Total Environ. 835, 155470. https://doi.org/10.1016/j.scitotenv.2022.155470.

An, J.W., Kang, D.J., Tran, K.T., Kim, M.J., Lim, T., Tran, T., 2012. Recovery of lithium from Uyuni Salar brine. Hydrometallurgy 117–118, 64–70. https://doi.org/10.1016/j.hydromet.2012.02.008.

Araoka, D., Kawahata, H., Takagi, T., Watanabe, Y., Nishimura, K., Nishio, Y., 2014. Lithium and strontium isotopic systematics in playas in Nevada, USA: constraints on the origin of lithium. Mineral. Deposita 49, 371–379. https://doi.org/10.1007/s00126-013-0495-y.

Ávila Salas, C.A., 2023. Caracterización hidrogeoquímica de los Flujos de Agua subterránea Que Alimentan el Sistema hídrico del Salar de Pastos Grandes. Universidad Nacional de la Pampa, Argentina.

Bąbel, M., Schreiber, B.C., 2014. Geochemistry of evaporites and evolution of seawater. In: Treatise on Geochemistry. Elsevier, pp. 483–560. https://doi.org/10.1016/B978-0-08-095975-7.00718-X.

Badaut, D., Risacher, F., 1983. Authigenic smectite on diatom frustules in Bolivian saline lakes. Geochim. Cosmochim. Acta 47, 363–375. https://doi.org/10.1016/0016-7037(83)90259-4.

Baker, P.A., Rigsby, C.A., Seltzer, G.O., Fritz, S.C., Lowenstein, T.K., Bacher, N.P., Veliz, C., 2001. Tropical climate changes at millennial and orbital timescales on the Bolivian Altiplano. Nature 409, 698–701. https://doi.org/10.1038/35055524.

Ballivian, O., Risacher, F., 1981. Los Salares del Altiplano Boliviano Metodos de Estudio Y Estimanion Economica. Office de la Recherche Scientifique et Technique Outre-Mer, Paris.

Benison, K.C., 2019. The physical and chemical sedimentology of two High-Altitude acid Salars in Chile: sedimentary processes in an extreme environment. J. Sediment. Res. 89, 147–167. https://doi.org/10.2110/jsr.2019.9.

Bertin, D., Bustos, E., Grosse, P., Báez, W., 2025. The Central Andes of South America: a review of its tectono-magmatic evolution. J. S. Am. Earth Sci. 158, 105503. https://doi.org/10.1016/j.jsames.2025.105503.

Borda, L.G., Godfrey, L.V., Del Bono, D.A., Blanco, C., García, M.G., 2023. Low-temperature geochemistry of b in a hypersaline basin of Central Andes: insights from mineralogy and isotopic analysis (δ11B and 87Sr/86Sr). Chem. Geol. 635, 121620. https://doi.org/10.1016/j.chemgeo.2023.121620.

Boschetti, T., Cortecci, G., Barbieri, M., Mussi, M., 2007. New and past geochemical data on fresh to brine waters of the Salar de atacama and andean altiplano, northern Chile. Geofluids 7, 33–50. https://doi.org/10.1111/j.1468-8123.2006.00159.x.

Boschetti, T., Salvioli-Mariani, E., Toscani, L., 2024. Lithium-rich basement brines: activity versus concentration geothermometry. Geothermics 119, 102965. https://doi.org/10.1016/j.geothermics.2024.102965.

Bougeault, C., Durlet, C., Vennin, E., Muller, E., Ader, M., Ghaleb, B., Gérard, E., Virgone, A., Gaucher, E.C., 2020. Variability of carbonate isotope signatures in a hydrothermally influenced system: insights from the Pastos Grandes caldera (Bolivia). Minerals 10, 989. https://doi.org/10.3390/min10110989.

Bradley, D., Munk, L., Jochens, H., Hynek, S., Labay, K., 2013. A preliminary Deposit Model for Lithium Brines (no. 2013–1006). In: U.S. Geological Survey Open-File Report. U.S. Geological Survey.

Bryan, S.P., Marchitto, T.M., 2008. Mg/Ca–temperature proxy in benthic foraminifera: new calibrations from the Florida straits and a hypothesis regarding Mg/Li. Paleoceanography 23. https://doi.org/10.1029/2007PA001553.

Case, D.H., Robinson, L.F., Auro, M.E., Gagnon, A.C., 2010. Environmental and biological controls on mg and li in deep-sea Scleractinian corals. Earth Planet. Sci. Lett. 300, 215–225. https://doi.org/10.1016/j.epsl.2010.09.029.

Chen, C., Lee, C.-T.A., Tang, M., Biddle, K., Sun, W., 2020. Lithium systematics in global arc magmas and the importance of crustal thickening for lithium enrichment. Nat. Commun. 11, 5313. https://doi.org/10.1038/s41467-020-19106-z.

Cioni, R., Marini, L., 2020. A Thermodynamic Approach to Water Geothermometry, Springer Geochemistry. Springer International Publishing, Cham. https://doi.org/10.1007/978-3-030-54318-1.

Coffey, D.M., Munk, L.A., Ibarra, D.E., Butler, K.L., Boutt, D.F., Jenckes, J., 2021. Lithium storage and release from lacustrine sediments: implications for lithium enrichment and sustainability in continental brines. Geochem. Geophys. Geosyst. 22. https://doi.org/10.1029/2021GC009916.

Cornejo, P., 1987. Hydrotermal alteration zones and Sulphur deposits in upper cenozoic vocanoes of Salar de Gorbea, Andes of northern Chile, 87. Pacific Rim Congress, pp. 877–885.

Cortecci, G., Boschetti, T., Mussi, M., Lameli, C.H., Mucchino, C., Barbieri, M., 2005. New chemical and original isotopic data on waters from El Tatio geothermal field, northern Chile. Geochem. J. 39, 547–571. https://doi.org/10.2343/geochemj.39.547.

Cortes-Calderon, E.A., Ellis, B.S., Tavazzani, L., Magna, T., Harris, C., Benson, T.R., 2025. Lithium inventory of the cerro Galán volcanic system (Argentina): the role of magmatism as a source for Li-Bearing brine deposits. Econ. Geol. 120, 1141–1165. https://doi.org/10.5382/econgeo.5154.

de Silva, S.L., 1989. Altiplano-Puna volcanic complex of the Central Andes. Geology 17, 1102–1106. https://doi.org/10.1130/0091-7613(1989)017%253C1102:APVCOT%253E2.3.CO;2.

de Silva, S., Zandt, G., Trumbull, R., Viramonte, J.G., Salas, G., Jiménez, N., 2006. Large ignimbrite eruptions and volcano-tectonic depressions in the Central Andes: a thermomechanical perspective. Geol. Soc. Lond. Spec. Publ. 269, 47–63. https://doi.org/10.1144/GSL.SP.2006.269.01.04.

Del Bono, D.A., Borda, L.G., Godfrey, L.V., Chiaramonte, N.L., Balbis, C., Pasquini, A.I., García, M.G., 2026. Mineralogical and chemical transformations of volcanic ash and rocks through interaction with water: insights into the genesis of lithium deposits in Puna brines. Mineral. Deposita. https://doi.org/10.1007/s00126-026-01428-5.

Dellinger, M., West, A.J., Paris, G., Adkins, J.F., Pogge von Strandmann, P.A.E., Ullmann, C.V., Eagle, R.A., Freitas, P., Bagard, M.-L., Ries, J.B., Corsetti, F.A., Perez-Huerta, A., Kampf, A.R., 2018. The Li isotope composition of marine biogenic carbonates: patterns and mechanisms. Geochim. Cosmochim. Acta 236, 315–335. https://doi.org/10.1016/j.gca.2018.03.014. Chemistry of Oceans Past and Present: A Special Issue in Tribute to Harry Elderfield.

Desaulty, A.-M., Monfort Climent, D., Lefebvre, G., Cristiano-Tassi, A., Peralta, D., Perret, S., Urban, A., Guerrot, C., 2022. Tracing the origin of lithium in li-ion batteries using lithium isotopes. Nat. Commun. 13, 4172. https://doi.org/10.1038/s41467-022-31850-y.

Drever, J.I., 1997. The Geochemistry of Natural Waters: Surface and Groundwater Environments, 3rd ed. Prentice Hall.

Ducea, M.N., DeCelles, P.G., Chapman, J.B., Delph, J.R., Carrapa, B., Petrescu, L., Ward, K.M., Rossel, P., 2026. The role of crustal magmatism in the formation and the evolution of orogenic plateaus. GSA Bull. https://doi.org/10.1130/B38190.1.

Ellis, B.S., Szymanowski, D., Magna, T., Neukampf, J., Dohmen, R., Bachmann, O., Ulmer, P., Guillong, M., 2018. Post-eruptive mobility of lithium in volcanic rocks. Nat. Commun. 9, 3228. https://doi.org/10.1038/s41467-018-05688-2.

Ellis, B.S., Szymanowski, D., Harris, C., Tollan, P.M.E., Neukampf, J., Guillong, M., Cortes-Calderon, E.A., Bachmann, O., 2022. Evaluating the potential of Rhyolitic glass as a lithium source for brine deposits. Econ. Geol. 117, 91–105. https://doi.org/10.5382/econgeo.4866.

Ericksen, G.E., Salas, R., 1987. Geology and Resources of the Salars in the Central Andes (Open-File Report No. 88–210), Open-File Report. U.S. Geological Survey.

Ericksen, G.E., Vine, J.D., Raul Ballón, A., 1978. Chemical composition and distribution of lithium-rich brines in Salar de Uyuni and nearby Salars in southwestern Bolivia. Energy 3, 355–363. https://doi.org/10.1016/0360-5442(78)90032-4.

Eugster, H.P., Hardie, L.A., 1978. Saline Lakes. In: Lerman, A. (Ed.), Lakes: Chemistry, Geology, Physics. Springer, New York, NY, pp. 237–293. https://doi.org/10.1007/978-1-4757-1152-3_8.
Freymuth, H., Brandmeier, M., Wörner, G., 2015. The origin and crust/mantle mass balance of central Andean ignimbrite magmatism constrained by oxygen and strontium isotopes and erupted volumes. Contrib. Mineral. Petrol. 169, 58. https://doi.org/10.1007/s00410-015-1152-5.
Gamboa, C., Godfrey, L., Herrera, C., Custodio, E., Soler, A., 2019. The origin of solutes in groundwater in a hyper-arid environment: a chemical and multi-isotope approach in the Atacama desert, Chile. Sci. Total Environ. 690, 329–351. https://doi.org/10.1016/j.scitotenv.2019.06.356.
Garcia, M.G., Borda, L.G., Godfrey, L.V., López Steinmetz, R.L., Losada-Calderon, A., 2020. Characterization of lithium cycling in the Salar de Olaroz, Central Andes, using a geochemical and isotopic approach. Chem. Geol. 531, 119340. https://doi.org/10.1016/j.chemgeo.2019.119340.
Giggenbach, W.F., 1978. The isotopic composition of waters from the el tatio geothermal field, northern Chile. Geochim. Cosmochim. Acta 42, 979–988. https://doi.org/10.1016/0016-7037(78)90287-9.
Giggenbach, W.F., 1988. Geothermal solute equilibria. Derivation of Na-K-Mg-Ca geoindicators. Geochim. Cosmochim. Acta 52, 2749–2765. https://doi.org/10.1016/0016-7037(88)90143-3.
Godfrey, L., Álvarez-Amado, F., 2020. Volcanic and saline lithium inputs to the Salar de atacama. Minerals 10, 201. https://doi.org/10.3390/min10020201.
Godfrey, L.V., Chan, L.-H., Alonso, R.N., Lowenstein, T.K., McDonough, W.F., Houston, J., Li, J., Bobst, A., Jordan, T.E., 2013. The role of climate in the accumulation of lithium-rich brine in the Central Andes. Appl. Geochem. 38, 92–102. https://doi.org/10.1016/j.apgeochem.2013.09.002.
Godfrey, L.V., Herrera, C., Gamboa, C., Mathur, R., 2019. Chemical and isotopic evolution of groundwater through the active Andean arc of northern Chile. Chem. Geol. 518, 32–44. https://doi.org/10.1016/j.chemgeo.2019.04.011.
Grove, M.J., Baker, P.A., Cross, S.L., Rigsby, C.A., Seltzer, G.O., 2003. Application of strontium isotopes to understanding the hydrology and paleohydrology of the Altiplano, Bolivia–Peru. Palaeogeogr. Palaeoclimatol. Palaeoecol. 194, 281–297. https://doi.org/10.1016/S0031-0182(03)00282-7. Late-quaternary palaeoclimates of the southern tropical Andes and adjacent regions.
Haferburg, G., Gröning, J.A.D., Schmidt, N., Kummer, N.-A., Erquicia, J.C., Schlömann, M., 2017. Microbial diversity of the hypersaline and lithium-rich Salar de Uyuni, Bolivia. Microbiol. Res. 199, 19–28. https://doi.org/10.1016/j.micres.2017.02.007.
Hardie, L.A., Eugster, H.P., 1970. The evolution of closed-basin brines. Mineral. Soc. Am. Spec. Pap. 3, 273–290.
Hofstra, A.H., Todorov, T.I., Mercer, C.N., Adams, D.T., Marsh, E.E., 2013. Silicate melt inclusion evidence for extreme pre-eruptive enrichment and post-eruptive depletion of lithium in silicic volcanic rocks of the western United States: implications for the origin of Lithium-Rich brines*. Econ. Geol. 108, 1691–1701. https://doi.org/10.2113/econgeo.108.7.1691.
Ibarra, F., Prezzi, C.B., 2019. The thermo-mechanical state of the Andes in the Altiplano-Puna region: insights from curie isotherm and effective elastic thickness determination. Rev. Asoc. Geol. Argent. 76, 352–362.
Ide, F., 1978. Cubicacion del Yacimiento Salar de Atacama. Universidad de Chile.
IEA, 2021. The Role of Critical Minerals in Clean Energy Transitions. International Energy Agency, Paris.
Inostroza, M., Godoy, Y., Donoso-Peña, M., Tassi, F., Aguilera, F., Capecchiacci, F., Rizzo, A.L., 2025. Geochemical survey of thermal springs from the Atacama region, northern Chile. J. Volcanol. Geotherm. Res. 467, 108411. https://doi.org/10.1016/j.jvolgeores.2025.108411.
Jaskula, B.W., 2025a. Lithium, Mineral Commodity Summaries 2025. U.S. Geological Survey. https://doi.org/10.3133/mcs2025.
Jaskula, B.W., 2025b. Lithium (2022 Minerals Yearbook). U.S. Geological Survey.
Jones, B., Renaut, R.W., 1994. Crystal fabrics and microbiota in large Pisoliths from Laguna Pastos Grandes, Bolivia. Sedimentology 41, 1171–1202. https://doi.org/10.1111/j.1365-3091.1994.tb01448.x.
Karmanocky III, F.J., Benison, K.C., 2016. A fluid inclusion record of magmatic/hydrothermal pulses in acid Salar ignorado gypsum, northern Chile. Geofluids 16, 490–506. https://doi.org/10.1111/gfl.12171.
Kasemann, S.A., Meixner, A., Erzinger, J., Viramonte, J.G., Alonso, R.N., Franz, G., 2004. Boron isotope composition of geothermal fluids and borate minerals from Salar deposits (Central Andes/NW Argentina). J. S. Am. Earth Sci. 16, 685–697. https://doi.org/10.1016/j.jsames.2003.12.004.
Kesler, S.E., Gruber, P.W., Medina, P.A., Keoleian, G.A., Everson, M.P., Wallington, T.J., 2012. Global lithium resources: relative importance of pegmatite, brine and other deposits. Ore Geol. Rev. 48, 55–69. https://doi.org/10.1016/j.oregeorev.2012.05.006.
Kharaka, Y.K., Mariner, R.H., 1989. Chemical geothermometers and their application to formation waters from sedimentary Basins. In: Thermal History of Sedimentary Basins. Springer, New York, NY, pp. 99–117. https://doi.org/10.1007/978-1-4612-3492-0_6.
Lagos Durán, L.V., 2016. Hidrogeoquímica de Fuentes Termales en Ambientes Salinos Relacionados Con Salares en los Andes del Norte de Chile. Universidad de Chile.
Lehner, B., Verdin, K., Jarvis, A., 2008. New global hydrography derived from spaceborne elevation data. EOS Trans. Am. Geophys. Union 89, 93–94. https://doi.org/10.1029/2008EO100001.
Lima-Quispe, N., Ruelland, D., Rabatel, A., Lavado-Casimiro, W., Condom, T., 2025. Modeling lake titicacas water balance: the dominant roles of precipitation and evaporation. Hydrol. Earth Syst. Sci. 29, 655–682. https://doi.org/10.5194/hess-29-655-2025.
Liu, M., Kong, Y., Guo, Q., 2025. Sources and enrichment mechanisms of lithium, rubidium, and cesium in waters of magmatic-hydrothermal systems. Earth Sci. Rev. 270, 105241. https://doi.org/10.1016/j.earscirev.2025.105241.
López Steinmetz, R.L., 2017. Lithium- and boron-bearing brines in the Central Andes: exploring hydrofacies on the eastern puna plateau between 23° and 23°30′S. Mineral. Deposita 52, 35–50. https://doi.org/10.1007/s00126-016-0656-x.
López Steinmetz, R.L., Salvi, S., 2021. Brine grades in andean salars: when basin size matters a review of the lithium triangle. Earth Sci. Rev. 217, 103615. https://doi.org/10.1016/j.earscirev.2021.103615.
López Steinmetz, R.L., Salvi, S., Gabriela García, M., Peralta Arnold, Y., Béziat, D., Franco, G., Constantini, O., Córdoba, F.E., Caffe, P.J., 2018. Northern Puna plateau-scale survey of li brine-type deposits in the Andes of NW Argentina. J. Geochem. Explor. 190, 26–38. https://doi.org/10.1016/j.gexplo.2018.02.013.
López Steinmetz, R.L., Salvi, S., Sarchi, C., Santamans, C., López Steinmetz, L.C., 2020. Lithium and brine geochemistry in the Salars of the southern Puna, Andean plateau of Argentina. Econ. Geol. 115, 1079–1096. https://doi.org/10.5382/econgeo.4754.
Lowenstein, T.K., Risacher, F., 2009. Closed basin brine evolution and the influence of Ca–Cl inflow waters: death valley and Bristol dry Lake California, Qaidam basin, China, and Salar de Atacama, Chile. Aquat. Geochem. 15, 71–94. https://doi.org/10.1007/s10498-008-9046-z.
Mamani, M., Wörner, G., Sempere, T., 2010. Geochemical variations in igneous rocks of the central Andean orocline (13°S to 18°S): tracing crustal thickening and magma generation through time and space. GSA Bull. 122, 162–182. https://doi.org/10.1130/B26538.1.
McCaffrey, M.A., Lazar, B., Holland, H.D., 1987. The evaporation path of seawater and the coprecipitation of br- and k+ with halite. J. Sediment. Res. 57, 928–937. https://doi.org/10.1306/212F8CAB-2B24-11D7-8648000102C1865D.
Meixner, A., Alonso, R.N., Lucassen, F., Korte, L., Kasemann, S.A., 2022. Lithium and Sr isotopic composition of Salar deposits in the Central Andes across space and time: the Salar de Pozuelos, ARGENTINA. Mineral. Deposita 57, 255–278. https://doi.org/10.1007/s00126-021-01062-3.
Meshram, P., Pandey, B.D., Mankhand, T.R., 2014. Extraction of lithium from primary and secondary sources by pre-treatment, leaching and separation: a comprehensive review. Hydrometallurgy 150, 192–208. https://doi.org/10.1016/j.hydromet.2014.10.012.
Mihalasky, M.J., Briggs, D.A., Baker, M., Jaskula, B., Cheriyan, K., Deloach-Overton, S. W., 2020. Lithium occurrences and processing facilities of Argentina, and Salars of the lithium triangle, Central South America. https://doi.org/10.5066/P9RLUH4F.
Millot, R., Scaillet, B., Sanjuan, B., 2010. Lithium isotopes in island arc geothermal systems: Guadeloupe, Martinique (French West Indies) and experimental approach. Geochim. Cosmochim. Acta 74, 1852–1871. https://doi.org/10.1016/j.gca.2009.12.007.
Mojid, M.R., Lee, K.J., You, J., 2024. A review on advances in direct lithium extraction from continental brines: ion-sieve adsorption and electrochemical methods for varied Mg/Li ratios. Sustain. Mater. Technol. 40, e00923. https://doi.org/10.1016/j.susmat.2024.e00923.
Moon, J.W., 2025. The Mineral Industry of China, 2022 Minerals Yearbook. U.S. Geological Survey.
Moraga, A., Chong, G., Fortt, M.A., Henriquez, H., 1974. Estudio Geologico del Salar de Atacama, Provincia de Antofagasta (Boletin). Instituto de Investigaciones Geologicas.
Morteani, G., Möller, P., Dulski, P., Preinfalk, C., 2014. Major, trace element and stable isotope composition of water and muds precipitated from the hot springs of Bolivia: are the waters of the springs potential ore forming fluids? Geochemistry 74, 49–62. https://doi.org/10.1016/j.chemer.2013.06.002.
Muller, E., Gaucher, E.C., Durlet, C., Moquet, J.S., Moreira, M., Rouchon, V., Louvat, P., Bardoux, G., Noirez, S., Bougeault, C., Vennin, E., Gérard, E., Chavez, M., Virgone, A., Ader, M., 2020. The origin of continental carbonates in Andean salars: a multi-tracer geochemical approach in Laguna Pastos Grandes (Bolivia). Geochim. Cosmochim. Acta 279, 220–237. https://doi.org/10.1016/j.gca.2020.03.020.
Munk, L.A., Boutt, D.F., Hynek, S.A., Moran, B.J., 2018. Hydrogeochemical fluxes and processes contributing to the formation of lithium-enriched brines in a hyper-arid continental basin. Chem. Geol. 493, 37–57. https://doi.org/10.1016/j.chemgeo.2018.05.013.
Munk, L.A., Boutt, D.F., Moran, B.J., McKnight, S.V., Jenckes, J., 2021. Hydrogeologic and geochemical distinctions in Freshwater-Brine systems of an Andean Salar. Geochem. Geophys. Geosyst. 22, e2020GC009345. https://doi.org/10.1029/2020GC009345.
Munk, L.A., Boutt, D., Butler, K., Russo, A., Jenckes, J., Moran, B., Kirshen, A., 2025. Lithium brines: origin, characteristics, and global distribution. Econ. Geol. 120, 575–597. https://doi.org/10.5382/econgeo.5134.
Munoz-Saez, C., Manga, M., Hurwitz, S., 2018. Hydrothermal discharge from the El Tatio Basin, Atacama, Chile. J. Volcanol. Geotherm. Res. 361, 25–35. https://doi.org/10.1016/j.jvolgeores.2018.07.007.
Nicholson, K., 1993. Geothermal Fluids Chemistry and Exploration Techniques. Springer, Berlin, Heidelberg. https://doi.org/10.1007/978-3-642-77844-5.
Orris, G.J., 1995. Borate Deposits (Open-File Report No. 95–842). U.S. Geological Survey.
Peralta Arnold, Y., Cabassi, J., Tassi, F., Caffe, P.J., Vaselli, O., 2017. Fluid geochemistry of a deep-seated geothermal resource in the Puna plateau (Jujuy province, Argentina). J. Volcanol. Geotherm. Res. 338, 121–134. https://doi.org/10.1016/j.jvolgeores.2017.03.030.
Placzek, C.J., 2005. Stratigraphy, Geochronology, and Geochemistry of Paleolakes on the Southern Bolivian Altiplano (Ph.D.). The University of Arizona.

Placzek, C.J., Quade, J., Patchett, P.J., 2011. Isotopic tracers of paleohydrologic change in large lakes of the Bolivian Altiplano. Quat. Res. 75, 231–244. https://doi.org/10.1016/j.yqres.2010.08.004.
Placzek, C.J., Quade, J., Patchett, P.J., 2013. A 130 ka reconstruction of rainfall on the Bolivian Altiplano. Earth Planet. Sci. Lett. 363, 97–108. https://doi.org/10.1016/j.epsl.2012.12.017.
Pueyo, J.J., Chong, G., Ayora, C., 2017. Lithium saltworks of the Salar de Atacama: a model for MgSO4-free ancient potash deposits. Chem. Geol. 466, 173–186. https://doi.org/10.1016/j.chemgeo.2017.06.005.
Pueyo, J.J., Demergasso, C., Escudero, L., Chong, G., Cortéz-Rivera, P., Sanjurjo-Sánchez, J., Carmona, V., Giralt, S., 2021. On the origin of saline compounds in acidic salt flats (Central Andean Altiplano). Chem. Geol. 574, 120155. https://doi.org/10.1016/j.chemgeo.2021.120155.
Reinoso Carbonell, V.V., Campodonico, V.A., Alasino, P.H., 2025. Origin of thermal waters in the fiambalá basin (Argentina): preliminary insights from hydrochemistry and isotopic tracers. Geothermics 132, 103434. https://doi.org/10.1016/j.geothermics.2025.103434.
Rettig, S.L., Jones, B.F., Risacher, F., 1980. Geochemical evolution of brines in the Salar of Uyuni, Bolivia. Chem. Geol. 57–79. https://doi.org/10.1016/0009-2541(80)90116-3.
Reyes, A.G., Trompetter, W.J., 2012. Hydrothermal water–rock interaction and the redistribution of li, b and cl in the Taupo volcanic zone, New Zealand. Chem. Geol. 314–317, 96–112. https://doi.org/10.1016/j.chemgeo.2012.05.002.
Risacher, F., 1984. Origine des concentrations extrêmes en bore et en lithium dans les saumures de l'Altiplano bolivien. Compte Rendus de l'Académie des Sciences de Paris 2 (299), 701–706.
Risacher, F., 1992. Géochimie des lacs salés et croûtes de sel de l'altiplano bolivien. Sgeol 45, 135–214. https://doi.org/10.3406/sgeol.1992.1889.
Risacher, F., Eugster, H.P., 1979. Holocene Pisoliths and encrustations associated with spring-fed surface pools, Pastos Grandes, Bolivia. Sedimentology 26, 253–270. https://doi.org/10.1111/j.1365-3091.1979.tb00353.x.
Risacher, F., Fritz, B., 1991a. Geochemistry of Bolivian Salars, Lipez, Southern Altiplano: origin of solutes and brine evolution. Geochim. Cosmochim. Acta 55, 687–705. https://doi.org/10.1016/0016-7037(91)90334-2.
Risacher, F., Fritz, B., 1991b. Quaternary geochemical evolution of the Salars of Uyuni and Coipasa, central Altiplano, Bolivia. Chem. Geol. 211–231. https://doi.org/10.1016/0009-2541(91)90101-V.
Risacher, F., Fritz, B., 2009. Origin of salts and brine evolution of Bolivian and Chilean Salars. Aquat. Geochem. 15, 123–157. https://doi.org/10.1007/s10498-008-9056-x.
Risacher, F., Alonso, H., Salazar, C., 1999. Geoquímica en Cuencas Cerradas: vol. I, II y III (No. 51). Convenio de Cooperación DGA-UCN-Orstom, Santiago.
Risacher, F., Alonso, H., Salazar, C., 2002. Hydrochemistry of two adjacent acid saline lakes in the Andes of northern Chile. Chem. Geol. 187, 39–57. https://doi.org/10.1016/S0009-2541(02)00021-9.
Risacher, F., Alonso, H., Salazar, C., 2003. The origin of brines and salts in Chilean salars: a hydrochemical review. Earth Sci. Rev. 63, 249–293. https://doi.org/10.1016/S0012-8252(03)00037-0.
Risacher, F., Fritz, B., Hauser, A., 2011. Origin of components in Chilean thermal waters. J. S. Am. Earth Sci. 31, 153–170. https://doi.org/10.1016/j.jsames.2010.07.002.
Rissmann, C., Leybourne, M., Benn, C., Christenson, B., 2015. The origin of solutes within the groundwaters of a high Andean aquifer. Chem. Geol. 396, 164–181. https://doi.org/10.1016/j.chemgeo.2014.11.029.
Rudnick, R.L., Gao, S., 2014. Composition of the Continental Crust. In: Treatise on Geochemistry. Elsevier, pp. 1–51. https://doi.org/10.1016/B978-0-08-095975-7.00301-6.
Sanjuan, B., Gourcerol, B., Millot, R., Rettenmaier, D., Jeandel, E., Rombaut, A., 2022. Lithium-rich geothermal brines in Europe: an up-date about geochemical characteristics and implications for potential Li resources. Geothermics 101, 102385. https://doi.org/10.1016/j.geothermics.2022.102385.
Sarchi, C., Lucassen, F., Meixner, A., Caffe, P.J., Becchio, R., Kasemann, S.A., 2023. Lithium enrichment in the Salar de Diablillos, Argentina, and the influence of cenozoic volcanism in a basin dominated by paleozoic basement. Mineral. Deposita 58, 1351–1370. https://doi.org/10.1007/s00126-023-01181-z.
Scandiffio, G., Alvarez, M., 1990. Informe geoquimico sobre la zona geotermica de Laguna Colorada, Bolivia (No. IAEA-TECDOC-641). In: Geothermal Investigations with Isotope and Geochemical Techniques in Latin America. IAEA, San José, Costa Rica.
Scandiffio, G., Cassis, W., 1990. Geochemical Report on the Emprexa Geothermal Area, Bolivia (No. IAEA-TECDOC-641). In: Geothermal Investigations with Isotope and Geochemical Techniques in Latin America. IAEA, San José, Costa Rica.
Scandiffio, G., Rodriguez, J., 1990. Geochemical Report on the Sajama Geothermal Area, Bolivia (No. IAEA-TECDOC-641). In: Geothermal Investigations with Isotope and Geochemical Techniques in Latin America. IAEA, San José, Costa Rica.
Schmidt, N., 2010. Hydrogeological and hydrochemical investigations at the Salar de Uyuni (Bolivia) with regard to the extraction of lithium. Freiberg Online Geol. 26, 101.
Schmidt, K., Oeser, M., Stechern, A., Ostertag-Henning, C., 2025. Hydrothermal experiments at in-situ conditions to identify li release reactions by water-mineral interactions in deep sedimentary basins of the north German Basin and upper Rhine Graben. Appl. Geochem. 195, 106622. https://doi.org/10.1016/j.apgeochem.2025.106622.
Schmitt, A.K., Kasemann, S., Meixner, A., Rhede, D., 2002. Boron in central Andean ignimbrites: implications for crustal boron cycles in an active continental margin. Chem. Geol. 183, 333–347. https://doi.org/10.1016/S0009-2541(01)00382-5.
Schnurr, W.B.W., Trumbull, R.B., Clavero, J., Hahne, K., Siebel, W., Gardeweg, M., 2007. Twenty-five million years of silicic volcanism in the southern central volcanic zone of the Andes: geochemistry and magma genesis of ignimbrites from 25 to 27°s, 67 to 72°w. J. Volcanol. Geotherm. Res. 166, 17–46. https://doi.org/10.1016/j.jvolgeores.2007.06.005.
Servant-Vildary, S., Roux, M., 1990. Multivariate analysis of diatoms and water chemistry in Bolivian saline lakes. Hydrobiologia 197, 267–290. https://doi.org/10.1007/BF00026956.
Sieland, R., 2014. Hydraulic investigations of the Salar de Uyuni, Bolivia. Freiberg Online Geol. 37, 208.
Sieland, R., Schmidt, N., Schön, A., Schreckenbach, J., Merkel, B., 2011. Geochemische, hydrogeologische und feinstratigraphische Untersuchungen am Salar de Uyuni (Bolivien). TU Bergakademie Freiberg, Freiberg.
Stringfellow, W.T., Dobson, P.F., 2021. Technology for the recovery of lithium from geothermal brines. Energies 14, 6805. https://doi.org/10.3390/en14206805.
Suosaari, E.P., Lascu, I., Oehlert, A.M., Parlanti, P., Mugnaioli, E., Gemmi, M., Machabee, P.F., Piggot, A.M., Palma, A.T., Reid, R.P., 2022a. Authigenic clays as precursors to carbonate precipitation in saline lakes of Salar de Llamara, Northern Chile. Commun. Earth Environ. 3, 325. https://doi.org/10.1038/s43247-022-00658-5.
Suosaari, E.P., Oehlert, A.M., Lascu, I., Decho, A.W., Piggot, A.M., Palma, A.T., Machabee, P.F., Reid, R.P., 2022b. Environmental and biological controls on sedimentary bottom types in the Puquios of the Salar de Llamara, Northern Chile. Geosciences 12. https://doi.org/10.3390/geosciences12060247.
Suosaari, E.P., Dupraz, C., Oehlert, A.M., Lascu, I., Vitek, B.E., Piggot, A.M., Palma, A.T., Reid, R.P., 2026. Coupled authigenic mg silicate and carbonate precipitation in saline lakes of the Salar de Atacama, Northern Chile. Depositional Rec. 12, e70055. https://doi.org/10.1002/dep2.70055.
Tassi, F., Aguilera, F., Darrah, T., Vaselli, O., Capaccioni, B., Poreda, R.J., Delgado Huertas, A., 2010. Fluid geochemistry of hydrothermal systems in the Arica-Parinacota, Tarapacá and Antofagasta regions (northern Chile). J. Volcanol. Geotherm. Res. 192, 1–15. https://doi.org/10.1016/j.jvolgeores.2010.02.006.
Tosca, N.J., Tutolo, B.M., 2023. How to make an alkaline lake: fifty years of chemical divides. Elements 19, 15–21. https://doi.org/10.2138/gselements.19.1.15.
Tutolo, B.M., Tosca, N.J., 2018. Experimental examination of the mg-silicate-carbonate system at ambient temperature: implications for alkaline chemical sedimentation and lacustrine carbonate formation. Geochim. Cosmochim. Acta 225, 80–101. https://doi.org/10.1016/j.gca.2018.01.019.
Vigier, N., Decarreau, A., Millot, R., Carignan, J., Petit, S., France-Lanord, C., 2008. Quantifying Li isotope fractionation during Smectite formation and implications for the li cycle. Geochim. Cosmochim. Acta 72, 780–792. https://doi.org/10.1016/j.gca.2007.11.011.
Vignoni, P.A., Jurikova, H., Schröder, B., Tjallingii, R., Córdoba, F.E., Lecomte, K.L., Pinkerneil, S., Grudzinska, I., Schleicher, A.M., Viotto, S.A., Santamans, C.D., Rae, J. W.B., Brauer, A., 2024. On the origin and processes controlling the elemental and isotopic composition of carbonates in hypersaline Andean lakes. Geochim. Cosmochim. Acta 366, 65–83. https://doi.org/10.1016/j.gca.2023.11.032.
Williams, G.D.Z., Vengosh, A., 2025. Quality of wastewater from Lithium-Brine mining. Environ. Sci. Technol. Lett. 12, 151–157. https://doi.org/10.1021/acs.estlett.4c01124.
Williams, G.D.Z., Nativ, P., Vengosh, A., 2025a. The role of boron in controlling the pH of lithium brines. Sci. Adv. 11, eadw3268. https://doi.org/10.1126/sciadv.adw3268.
Williams, G.D.Z., Petrović, M., Hill, R.C., Hall, G.A., Vengosh, A., 2025b. The water quality impacts of legacy Hard-Rock lithium mining and processing. Environ. Sci. Technol. 59, 16492–26505. https://doi.org/10.1021/acs.est.5c13682.
Williams, G.D.Z., Barre, J., Louvat, P., Bérail, S., Millot, R., Vengosh, A., 2026. Geochemical controls on the formation of lithium brines in closed-basins of the lithium triangle. Earth Planet. Sci. Lett. 679, 119849. https://doi.org/10.1016/j.epsl.2026.119849.
Wimpenny, J., James, R.H., Burton, K.W., Gannoun, A., Mokadem, F., Gíslason, S.R., 2010. Glacial effects on weathering processes: new insights from the elemental and lithium isotopic composition of West Greenland rivers. Earth Planet. Sci. Lett. 290, 427–437. https://doi.org/10.1016/j.epsl.2009.12.042.
Wimpenny, J., Colla, C.A., Yu, P., Yin, Q.-Z., Rustad, J.R., Casey, W.H., 2015. Lithium isotope fractionation during uptake by gibbsite. Geochim. Cosmochim. Acta 168, 133–150. https://doi.org/10.1016/j.gca.2015.07.011.
Yang, S., Wang, Y., Pan, H., He, P., Zhou, H., 2024. Lithium extraction from low-quality brines. Nature 636, 309–321. https://doi.org/10.1038/s41586-024-08117-1.
YLB, 2019. Memoria Institucional 2019. Yacimientos de Litio Bolivianos.
Yuan, X., Hu, Y., Zhao, Y., Li, Q., liu, C., 2021. Contribution of hydrothermal processes to the enrichment of lithium in brines: evidence from water–rock interacting experiments. Aquat. Geochem. 27, 221–239. https://doi.org/10.1007/s10498-021-09395-1.
Zheng, M., Liu, X., 2009. Hydrochemistry of salt lakes of the Qinghai-Tibet plateau, China. Aquat. Geochem. 15, 293–320. https://doi.org/10.1007/s10498-008-9055-y.
Zhu, R., Wang, S., Srinivasakannan, C., Li, S., Yin, S., Zhang, L., Jiang, X., Zhou, G., Zhang, N., 2023. Lithium extraction from salt lake brines with high magnesium/lithium ratio: a review. Environ. Chem. Lett. 21, 1611–1626. https://doi.org/10.1007/s10311-023-01571-9.